Journal of Polymer Research (2020) 27: 182
https://doi.org/10.1007/s10965-020-02157-7

REVIEW PAPER

Recent advancements in manufacturing technologies of microcellular polymers: a review

Rupesh Dugad [1,2] · G. Radhakrishna [1,2] · Abhishek Gandhi [1,2]

Received: 7 January 2020 / Accepted: 8 May 2020 / Published online: 30 June 2020

Abstract

Significant research efforts are being pursued by numerous plastic foaming industries towards the transformation of macrocellular polymer foam to microcellular and imminent future is trending towards nanocellular polymer foams. These novel foamed plastic possess enhanced properties and easy tunability which could potentially fulfill many of the ever-evolving industrial requirements. These industrial requirements have led to several advancements in the current manufacturing technologies and as a result, new industrial-scale production technologies are being researched upon cellular plastics and its allied composites. The microcellular polymeric foams have huge industrial demand due to their improved properties such as specific strength, energy absorption, and thermal/electrical/acoustic insulation compared to their unfoamed counterparts. This review article aims to summarise the existing manufacturing technologies for producing microcellular polymers and provide an up-to-date report on the recent advancements in these manufacturing technologies.

Keywords Microcellular · Ultrasound-aided foaming · Bimodal foaming · EMI shielding · Wood fiber composites · Porous foam

Introduction

The polymer foaming transforms solid polymers into cellular structured polymeric composites by incorporation of a large number of very small-sized bubbles to reduce the use of material without a significant effect on the mechanical properties of the product. In the 1930s, the first polymer foam with macrocellular structure was reported [1], and since then the research & development is being consistently pursued towards the smaller cell types of cellular structure. In the 1980s, polymer foam with microcellular structure was reported by Prof. Suh et.al [2] from Massachusetts Institute of Technology and subsequently, in the early 2000s, the nanocellular polymeric structure came into existence. The development in this field of research still continues to endeavour through numerous cutting-edge innovation for several diverse industrial applications [1]. The microcellular plastics are being extensively used in a wide range of applications such as biomedical, automotive, naval, aerospace, safety goods, insulation purpose in construction, packaging, filters, membranes, cushioning owing to its properties like strength to weight ratio, toughness, insulating properties, flexibility, etc. [2–6]. These cellular materials can be classified according to the interconnectivity of cell structure, cell size, cell density, expansion ratio, elastic modulus [1, 7–10]. Figure 1 shows a clear depiction of the classification of foamed polymers.

✉ Rupesh Dugad
dugadrupesh23@gmail.com

[1] CIPET: School for Advanced Research in Polymers (SARP) - APDDRL, #488-B, 4th Floor, Block - 2, KIADB Building,14th Cross, Peenya 2nd Stage, Bengaluru, Karnataka 560058, India

[2] CIPET: School for Advanced Research in Polymers (SARP) - LARPM, B -25, CNI Complex, Bhubaneswar, Odisha 751024, India

Mechanism of polymer foaming

The mechanism of polymer foaming typically comprises three distinct stages which are clearly shown in Fig. 2 [1, 3, 11]. The first stage is the dissolution of gas or blowing agent. In this stage, a polymer sample (solid or melt) is loaded with a high-pressure blowing agent such as CO_2 or N_2. The dissolution of the blowing agent in the polymer matrix occurs over an extended period of time, till full saturation level is achieved. The dissolution process involves the mixing of two different phases (gas & solid) to form a single-phase homogenous solution. The dissolution of gas or blowing agent in polymer also causes plasticization effect which assists in the flow of polymer matrix during the foaming process. Plasticization

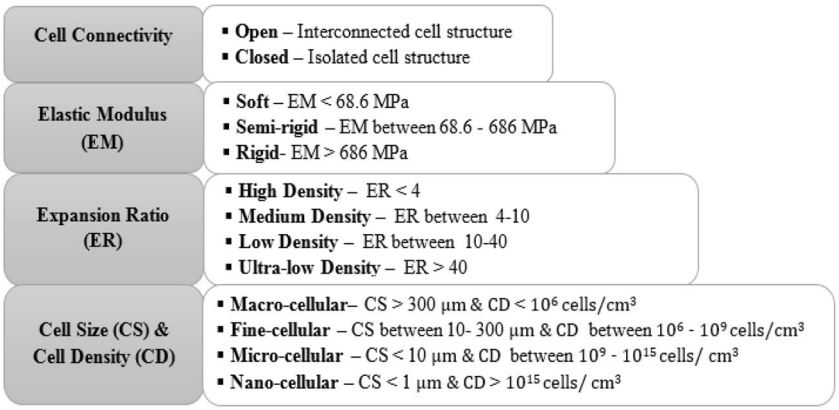

Fig. 1 Classification of foamed polymers

occurs due to the suppression of glass transition temperature & result in the decrease of stiffness, viscosity and increases the chain mobility of polymer materials which cause the reduction in energy barrier for cell nucleation [12]. The second stage is cell nucleation and cell growth. Thermodynamic instability is the basic principle behind cell nucleation. The thermodynamic instability can be induced either by a sudden rise in temperature or a sudden drop in pressure. Due to this thermodynamic instability, the solubility of CO_2 within the polymer matrix drops instantaneously and the dissolved blowing agent emerges out from the polymer matrix, thereby creating a large number of nuclei. Finally, the third stage is the cell stabilization stage. To preserve the so-developed cell structure, the foamed sample is quenched in water or other suitable cooling media. Even though after quenching, cell growth may continue.

The blowing agent plays an important role in the transformation of solid polymer into the cellular structured polymer. Two types of blowing agents are using generally in foam manufacturing namely,- chemical blowing agent (CBA) and physical blowing agent (PBA) [1, 5, 7, 13]. The foaming with PBA has many advantages over foaming with CBA, such as lesser materials usage, no residues, and lower cost. In foaming with PBA, mostly CO_2 or N_2 are used as blowing agent because of their inertness, easiness to integrate, availability, and notably low cost [14, 15]. The cell density is the function of saturation pressure [16]. The increase in saturation pressure increases the dissolution of the blowing agent within the polymer matrix & leads to higher cell density [17].

Traditional manufacturing technologies of microcellular polymers

The traditional techniques generally used for microcellular polymeric foam manufacturing are; batch solid-state microcellular foaming, extrusion foaming, and injection mould foaming. Out of which mostly extrusion foaming and injection mould foaming are commercially used for foam production and batch solid-state foaming is being used for research purposes.

Batch solid-state microcellular foaming

Batch solid-state foaming is a non-continuous foam formation technique as in this technique a saturation of the polymer sample and the foaming (i.e. cell nucleation and cell growth) occurs individually. The polymer sample to be foamed is in solid-state and is processed in batches/group in a closed vessel at defined saturation parameters, thus named as batch solid-state foaming [1, 3, 9, 12, 18]. The batch solid-state foaming process is further classified as- Pressure-induced (One-step) and Temperature-induced (Two-step). These two techniques are discussed in detail below.

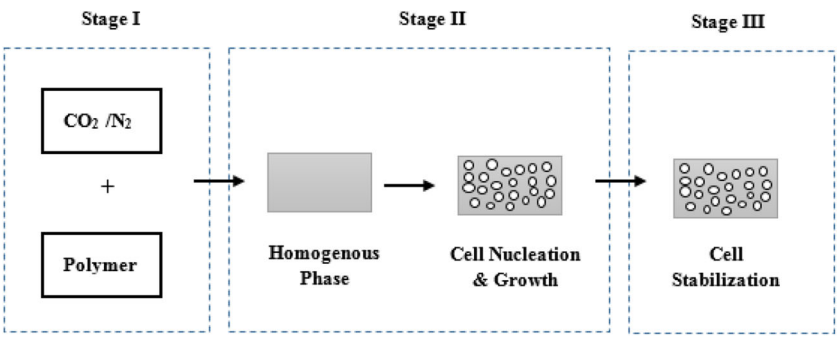

Fig. 2 Mechanism of polymer foaming

Pressure-induced (one-step) technique- In this technique, a solid polymer sample is placed inside an autoclave vessel, which is pressurized with blowing agent at high pressure termed as saturation pressure and at a certain temperature termed as saturation temperature for a defined period of time termed as saturation time. Once the polymer sample is fully saturated, the vessel is depressurized rapidly at a high depressurization rate. This gas saturated polymer at a fully saturated state which is defined as, the state above which no more dissolution or absorption of blowing agent in the polymer sample can occur. In this type of batch foaming method, the induction of thermodynamic instability occurs due to the high pressure gradient ($-\frac{\partial P}{\partial t}$) which results in cell nucleation and its subsequent growth. The negative sign indicates the drop in pressure with respect to time. Finally, the sample is cooled in water for stabilization of the microstructure [1, 3, 12, 19]. Figure 3 represents a schematic of the typical pressure-induced batch solid-state microcellular foaming process.

Temperature-induced (two-step) technique- In the temperature-induced technique, the sample saturation is typically done at a temperature lower than the glass transition temperature of the polymer matrix. Immediately after depressurization, the sample is taken out from the vessel and is dipped in a hot oil bath or glycerine/silicon bath [20, 21]. The bath temperature is generally kept above the glass transition temperature of the polymer matrix which is termed as foaming temperature. If the foaming temperature is above that glass transition temperature, stiffness or viscosity of polymer matrix decreases thus dissolved gas diffused out fastly and cause nucleation [22]. The time for which the saturated sample is dipped inside the hot bath is termed as the foaming time. In general, with an increase in the foaming temperature, the cell size also increases because higher temperature reduces the polymer viscosity and in turn reduces the resistance to cell growth [1, 4, 18]. In this type of batch foaming, the thermodynamic instability for cell nucleation and cell growth occurs due to the high temperature gradient ($+\frac{\partial T}{\partial t}$). The positive sign indicates the rise in temperature with respect to time. Figure 4 shows a schematic of the typical temperature-induced batch solid-state microcellular foaming process. Also, Table 1 depicts the comparison between techniques of batch solid-state microcellular foaming [1, 3, 4, 18, 22].

The limitation of batch solid-state microcellular foaming is that it takes a significant amount of processing time for the development of foam and the autoclave vessel capacity also limits its product dimensions. To overcome this drawback, processes like extrusion foaming and injection mould foaming were developed [22], which could manufacture microcellular foamed products at an industrial scale.

Extrusion microcellular foaming

Extrusion microcellular foaming was developed by amalgamating conventional polymer extrusion process and external gas injection system which could disperse the blowing agent within the polymer melt [1]. When compared with the batch foaming process, the extrusion foaming process provides higher productivity, ease of control, versatility in end-product properties and profiles [22]. In extrusion foaming, the polymer pellets are fed into the barrel through hopper. The pellets get melted inside the barrel due to high temperature and the blowing agent at high pressure from the external gas injection system is injected into polymer melt, typically in the compression zone of the extruder and action of shear forms a homogenous mixture.

Generally, two kinds of extrusion processes are used which are single barrel extrusion and tandem (two-barrel) extrusion. In the single barrel extrusion, melting and cooling polymer matrix occurs in the same barrel while in tandem extrusion, separate barrels are there for melting and cooling [1, 4, 7]. Significantly better results are obtained with tandem extrusion than single barrel extrusion but gas leakage possibility, setup cost & power consumption are more in tandem extrusion

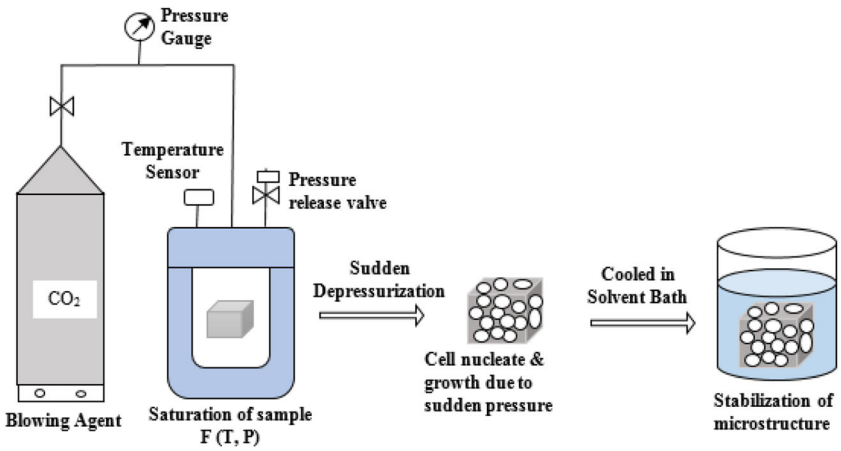

Fig. 3 Schematic representation of pressure-induced batch solid-state microcellular foaming

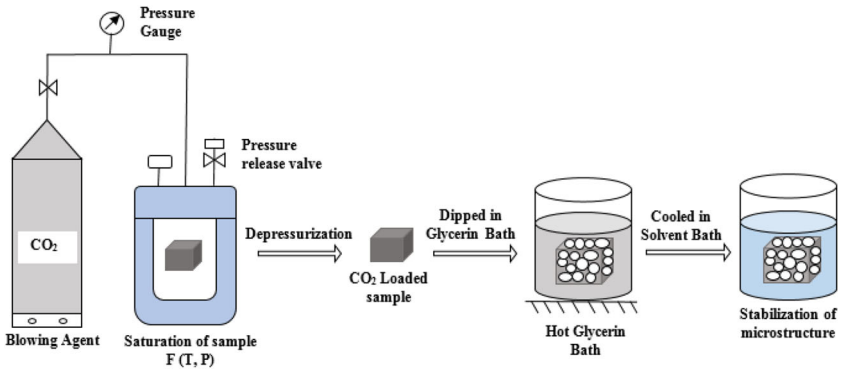

Fig. 4 Schematic representation of temperature-induced batch solid-state microcellular foaming

compared to single barrel extrusion [4, 7]. Figures 5 and 6 depict a typical schematic of single extrusion and tandem extrusion microcellular foaming.

The screw motion passes the molten mixture into the second barrel, here it gets cooled to a temperature lower than temperature in the first barrel. Further cooling provided to reduce the cell coalescence. The melt pump regulates the amount of molten mixture flowing through the extruder. As the molten mixture exits the extruder die head, a large number of cells begin to nucleate and subsequently grows. The primary driving force for this nucleation is thermodynamic instability due to the high pressure gradient ($-\frac{\partial P}{\partial t}$). The cell growth occurs until it stabilizes or ruptures [7, 23]. The dispersion of the blowing agent in polymer melts significantly affects the morphology of the developed foam using extrusion process. The blowing agent injecting location in extrusion barrel affects the residence time of blowing agent which in turn affects the morphology of the developed foam [24].

Injection mould microcellular foaming

In the injection mould microcellular foaming process, the polymer pellets get melted in the barrel and the blowing agent is mixed in the molten polymer to form a homogenous mixture. The screw pushes this single phase molten mixture and is injected in the mould, the pressure drops to the atmospheric pressure and this leads to the microcellular nucleation phenomenon. The nucleated cells grow till they are stabilized. Due to the presence of gas, plasticization of polymer chain occurs due to which the viscosity of melt decreases & it leads to decrease in injection pressure. Also, the lesser clamp force is required [11, 23, 25, 26], when compared with the conventional injection moulding process. Figure 7 shows the typical schematic setup for injection mould microcellular foaming.

The cycle time required for microcellular injection mould foaming is significantly lesser than conventional injection moulding. Approximately 20–50% cycle time can be saved with microcellular injection moulding. Figure 8 shows a comparison between conventional and microcellular injection foaming.

In microcellular injection foaming, the viscosity of polymer matrix reduced due to the presence of blowing agent (i.e. CO_2/ N_2) which increases the filling speed and reduced filling time. The packing pressure provided by gas in bubbles thus, holding time is almost eliminated. And as cell nucleation & growth required endothermic variation thus, cooling time is also reduced [13, 27]. Table 2 represents the comparison between traditional manufacturing processes of microcellular polymers [1, 3, 4].

Advanced manufacturing technologies in the microcellular foaming

From the last decade, a number of innovations have occurred in the manufacturing technologies of microcellular foam.

Table 1 Comparison between techniques of batch solid-state microcellular foaming

Comparative point	Pressure-induced technique	Temperature-induced technique
Alternate term	One-step or Batch foaming	Two-step
Saturation temperature	Typically higher than Tg	Less than Tg
Thermodynamic instability	Due to high pressure gradient ($-\frac{\partial P}{\partial t}$)	Due to high temperature gradient ($+\frac{\partial T}{\partial t}$)
Time inclusion for foam preparation	Typically 2–4 h	Typically 16–24 h
Crucial processing parameters	Saturation pressure, saturation temperature, depressurisation rate	Saturation time, foaming temperature, foaming time

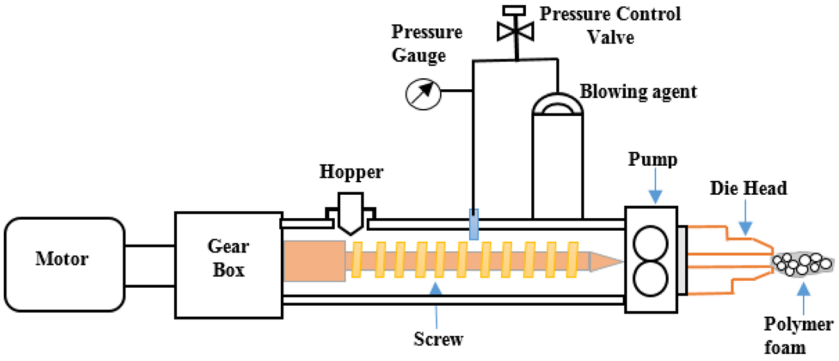

Fig. 5 Schematic representation of single barrel extrusion microcellular foaming

These advanced technologies include ultrasound-aided microcellular foaming, bi-modal microcellular foaming, and cyclic microcellular foaming. These advanced technologies are developed either by specific process integration or process modification or variation in the process parameters & their levels to obtain the desired foam structure.

Ultrasound-aided microcellular foaming

Ultrasound-aided microcellular foaming is the advanced foaming technique in which external ultrasound vibration applied within the existing traditional batch foaming process to enhance the cell morphology of the foamed product. This technique is useful to convert the closed cell structure to an open or interconnected cell structure. The main application of this technique could be in the field of tissue engineering scaffold as it is a solvent-free technique and therefore, the new tissue generation ability of biological cells remains unaffected [28–30]. Also, it could be utilized for filters and membrane preparation [31]. The various process parameters such as ultrasound frequency, exposure time of ultrasound, the intensity of ultrasound, temperature of water in the ultrasound aided microcellular foaming technique which significantly affects the cell morphology of polymer foam. Figure 9 shows the schematic representation of for ultrasound aided microcellular foaming setup used by Gandhi et al.

Mechanism of ultrasound aided microcellular foaming

The ultrasonication creates the vibrational sinusoidal wave in an elastic medium. During the positive half of the wave, the distance between the molecules of the medium decreases and during negative half that distance increases. When the wave vibration reaches to threshold or peak, it create bubbles that are termed as cavitation bubbles. With time, the size of cavitation bubbles increased, when it reached the critical size it explodes violently and thus creating the packets of energy called microjets. These microjets start continuously striking on the polymer surface that creates the hot spot. The hot spot is confined to a localized area, experience extreme high temperature and pressure about 5000 °C and 1000 atm [31–33], which induces high thermodynamic instability.

The significant effect of ultrasonication on cell morphology depends on when ultrasonication assists with traditional foaming technique, i.e. either at the beginning of nucleation or after nucleation.

Ultrasonication applied at beginning of nucleation- The ultrasonication creates a number of cavitation bubbles which collapse violently once bubbles reach their critical sizes and thus creates hot spots. The extreme conditions of hot spots generate high thermodynamic instability which leads to the nucleation of a large number of small cells i.e. cell density gets enhanced [33].

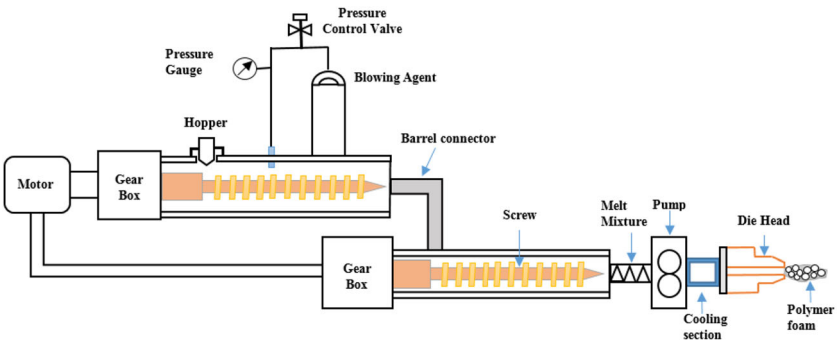

Fig. 6 Schematic representation of tandem extrusion microcellular foaming adapted from Ref [1] with kind permission from Elsevier

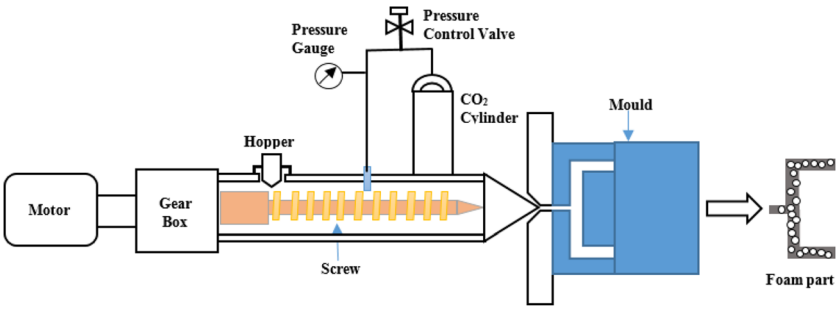

Fig. 7 Schematic representation of injection mould microcellular foaming adapted from Ref [1] with kind permission from Elsevier

Ultrasonication applied after cell nucleation & growth - The generated microjets continuously strike on the foam surface and break the surface cell walls. Then the water along with cavitation bubbles enters into inner foam. Further, in the same manner, cell walls get rupture and the interconnected or open cell structure achieved [33]. Even if there is heat generation at hot spots, it is consized to the localized area so that the overall temperature is less, and hence the foam shape or structure is not distorted [34]. The schematic representation of the mechanism of ultrasound aided microcellular foaming is shown in Fig.10.

Wang et al. demonstrated that ultrasound irradiation (UI) enhanced the non-uniform cell structure to uniform cell structure of the semi-crystalline or crystalline polymer if UI introduces at the beginning of cell nucleation. The delay in the introduction of UI leads to non-uniformity of structure and if the exposure time of UI increases, it leads to cell uniformity and enhances the cell density [28]. The literature review on ultrasound aided microcellular foaming is given in Table 3.

Bi-modal microcellular foaming

The bi-modal structure also termed as bi-cellular or complex cellular, as it consists of both large sized cells and small ones [40, 41]. The small sized cells provide mechanical strength, thermal insulation, whereas large sized cells provide low bulk density [42]. The bi-modal structured foam has better thermal insulation compared to uni-modal structured foam. The two different nucleating mechanisms are required to develop the bi-modal cell structure [42]. Generally, the bi-modal foam structure is developed by; two-step depressurization technique [43–51], co-blowing technique [40, 42, 52–54], polymer blend technique [55–58]. Along with this, some researchers developed bi-modal structure using ultrasound excitation [33], multiple soaking technique (MST) [59], temperature rising and depressurization [60], etc.

The schematic of two-step depressurization is shown in Fig. 11. In this technique initially, sample saturated at pressure (P_1) and temperature (T_1) for a defined time (t_1). Then depressurized the vessel to an intermediate pressure (P_2) and hold it for some time (t_2). Finally depressurized vessel to atmospheric pressure. This stepped depressurization causes large and small bubbles. The intermediate pressure also termed as holding pressure.

The co-blowing agent with a primary blowing agent also develops bi-modal cell structure. In this case, the different nucleating mechanism is induced by two different blowing agents. Generally, the large cell size is obtained by the co-blowing agent and small cell size is obtained by a primary blowing agent which may be due to the diffusion difference of blowing agent in the polymer matrix. The polymer blending technique leads to the formation of the bi-modal structure due to the non-homogeneity of polymer blend and also due to the difference in stiffness. This leads to time inclusion in first cell nucleation and second cell nucleation.

Gandhi et al. [33] shown that bi-modal structure could be created with ultrasound excitation in which the ultrasound frequency is a significant parameter that affects the bi-modal microcellular structure of ABS foam as shown in Fig. 12. The author found that the low ultrasound frequency (25 kHz) led to uniform cell morphology and high ultrasound frequency (45 kHz) led to bi-modal cell morphology. The high ultrasound frequency generated the number of microjets. These microjets continuously hit the polymer surface and formed a number of small cells. But microjets continued to strike the surface and forming new cells around the growing cells eventually which led to bi-modal microcellular morphology.

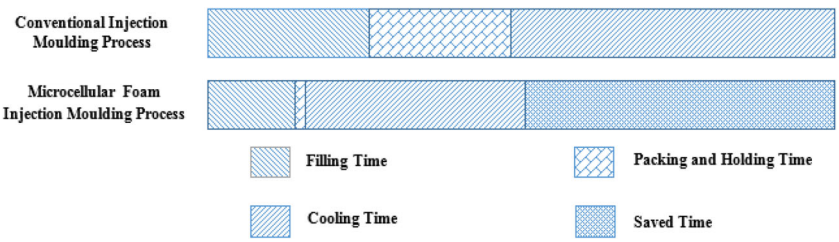

Fig. 8 Comparison between conventional and microcellular injection foaming adapted from Ref [13] under an open-access license

Table 2 Comparison between traditional manufacturing processes of microcellular polymers

Comparative point	Batch solid-state microcellular foaming	Extrusion microcellular foaming	Injection molding microcellular foaming
Type of process	Non-continuous	Continuous	Semi-continues
Sample state	Solid	Molten	Molten
Raw material required (amount)	Small	Large	Medium to large
Sample composition	Fixed	Variable	Variable
Blowing agent amount	More (upto saturation of sample)	As per requirement	As per requirement
Gas dissolution rate	Low	High	High
Cause of thermodynamic instability	$(+\frac{\partial T}{\partial t})$ or $(-\frac{\partial P}{\partial t})$	Only $(-\frac{\partial P}{\partial t})$	Only $(-\frac{\partial P}{\partial t})$
Processing time incurred	More	Moderate	Less
Size of sample	Small	Large	Moderate (depend on mould)
Skin formed	Thin	Medium Thicken	Thicker
Sample complexity	Simple	Simple	Both (simple & complex)
Variety of products	Moderate	Less	More
No. of temperature zones	One	More than one	More than one
Post-process	Final part dried	Final part calibrated and cut of the extruded foam	Final part calibrated or cut off the injected foam
Productivity	Low	High	High
Use	Lab Scale	Commercial	Commercial
Cost	Cheap	Expensive (depend on machine & mould standard)	Expensive(depend on machine & mould standard)

Huang et al. [59] developed another new technique called multiple soaking temperature (MST) to generate a bi-modal structure. In this method, first sample was sealed in the autoclave chamber at room temperature and pressurized with saturation pressure of P_1. Then raised temperature to T_1 which is the first soaking temperature, kept it for time t_1. After that, decreased the temperature to second soaking temperature T_2 kept for time t_2. Again temperature increased to third soaking temperature T_3 kept for time t_3, followed by a reduction in temperature to fourth soaking temperature or foaming temperature T_4 kept for time t_4, later depressurized chamber to ambient pressure. Finally cooled autoclave chamber to room temperature and foamed sample taken out from chamber. Here, soaking temperature array as $T_1 > T_3 > T_4 > T_2$. With this method, the author successfully fabricated porous bi-modal PLA foam with open-cell structure had porosity, open-cell content, average large and small cell size are 87.9%, 82.4%, 150 μm, and 8 μm respectively.

The thermodynamic instability could be generated by sudden pressure drop or sudden temperature rise which results in the cell nucleation and in general foaming process, either one of them is enough for nucleation. But Lin-Qiong Xu et al. [60] used both thermodynamic instability aspects synergistically and successfully created the bi-modal structure in polystyrene foam.

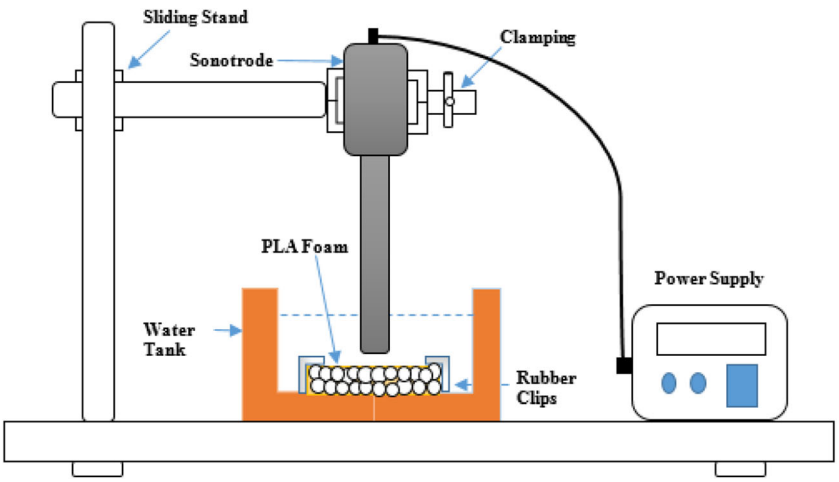

Fig. 9 Schematic of setup for ultrasound aided microcellular foaming- Adapted from Ref [29] with kind permission from Elsevier

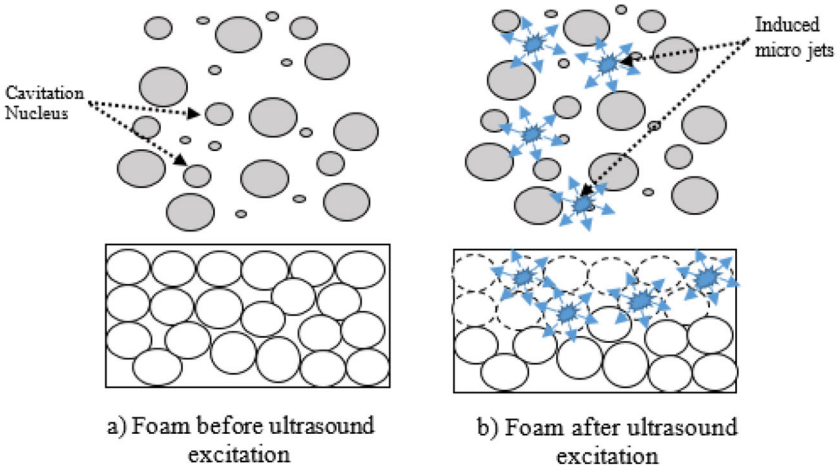

Fig. 10 Schematic representation of the mechanism of ultrasound aided microcellular foaming - Adapted from Ref [29] with kind permission from Elsevier

Table 3 Literature review on ultrasound aided microcellular foaming

Author	Material	Foaming process	Ultrasound treatment applied	Ultrasonic processor	Findings	Ref
Wang et al.	PLA	Batch Foaming	At very start of cell nucleation and at a time interval (0–20 s)	–	UI enhanced cell density about 2 orders of magnitude at different foaming temperatures.	[28]
Guo et al.	PLA	Batch Foaming	After PLA foam Cell nucleated	Sonics VCX750, Sonics & Materials Inc., USA, 20 kHz	Cell interconnectivity & permeability enhances with an intensity of ultrasound radiation.	[29]
Wang et al.	PLA	Batch Foaming	After PLA foam cells nucleated	VC750, Sonics Concept Inc., 20 kHz, 750 W	Ultrasound treatment changes closed cell to interconnected cell of size 30–90 μm.	[34]
Youn & H. Park	PU	Reaction Injection Moulding	After the imprignment mixing of two components	Piezo-electric actuator with titanium horn, 20 kHz	Negative pressure field generated by ultrasound which enhanced the nucleation rates.	[35]
Zhai et al.	PS	Batch Foaming	At the start of foaming	Ultrasound Irradiation	UI enhanced cell density about 100–1000 times & expansion ratio about 2–4 times	[36]
Wei Li et al.	PMMA	Selective Ultrasonic Foaming Process	At starting of PMMA foam cell nucleation	HIFU Transducer (H101 Sonic Concept Inc), 1.1 MHz, 200 W	Effect of scanning speed and ultrasound power on cell size were studied and cell size enhanced with the decrease in the scanning speed.	[30]
Wang et al.	PLA	Solid-State Foaming	After PLA foam cells nucleated	VC750 (20 kHz) & VC540 (40 kHz) Sonics & Materials, Inc) 750 W	Ultrasound effectiveness affected by pore size. Higher permeability achieved at a bigger pore size.	[31]
Byon & Youn	PS with ZnS and blend of PE wax & LDPE	Ultrasonic foaming	At the start of cell nucleation	Sonicor Model UP-400	Ultrasonic excitation enhanced nucleation with the generation of negative pressure.	[37]
Gandhi et al.	ABS	Batch foaming	At very starting of ABS foam cell nucleation	Martin-Walter push-pull transducer 25 and 45 kHz	Bi-modal cell structure at higher and uniform cell structure at lower sonication frequency was obtained.	[33]
Gandhi et al.	ABS	Cyclic Batch foaming	After ABS foam cells nucleated (second cycle)	Takashi Ultrasonics, 750 W 20 kHz	Ultra-low density porous ABS foam fabricated with the application of ultra-sound excitation.	[38]
Gandhi et al.	ABS	Batch foaming	Before the cell nucleation	Martin-Walter, Crest Ultrasonics MW1000GPI2 25 kHz, 1 kW	Distance of ultrasound transducer to sonication sample affects the cell nucleation.	[39]

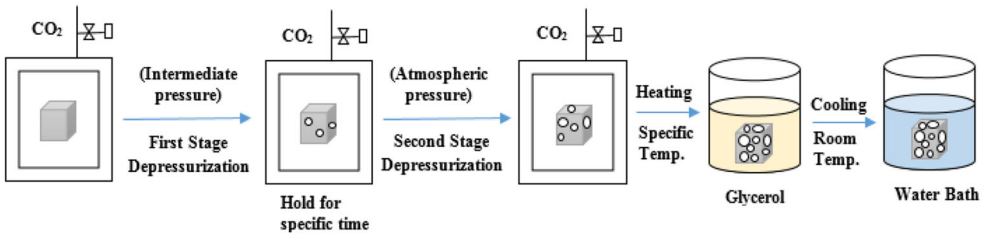

Fig. 11 Schematic representation of two-stage depressurization

Radhakrishna et al. used a step-wise depressurization technique (Four-step), and each depressurization step induced different nucleation phenomenon led in the development of bi-modal and multi-modal ABS foam microstructure [61].

The literature review on bi-modal microcellular foaming by two-step depressurization, co-blowing agent, polymer blend technique is given in Tables 4, 5, and 6 respectively.

Cyclic microcellular foaming

The cyclic foaming is repetitive foaming. In the cyclic foaming first, a neat polymer sample converts into a foamed sample then again foamed sample processed under the required levels of foaming parameters. From literature, it has seen that for cyclic microcellular foaming generally batch foaming process was used as; easy to control processing parameters and repeatability [65]. In the cyclic foaming process, saturation pressure is a crucial parameter; consider primary saturation pressure as P_1 and secondary saturation pressure as P_2. Also, the sequence of P_1 and P_2 plays a significant role in controlling cell morphology [65, 66]. Gandhi et al. developed a novel technique by applying the ultrasound assistance to cyclic foaming to produce ultralow density foam with interconnected cell structure as shown in Fig. 13. Table 7 shows the literature review on cyclic microcellular foaming.

Manufacturing technologies of advanced microcellular polymers

The microcellular polymers have enhanced properties owing to its micron-sized cell structure and therefore the application range gets widened compared to macron-sized cell structure. The advanced applications of the microcellular polymer such as EMI shielding, microcellular auxetic foam for sports & safety equipment, scaffolds for controlled drug released, wooden foam composites for high strength applications. The manufacturing technologies of advanced microcellular polymers, its properties and applications are discussed in detail.

Electromagnetic interference shielding microcellular polymers

The radiation generated by electronic devices interferes with each other causing the disruption in the functionality of devices is known as Electromagnetic Interference (EMI) [69, 70]. The ringing cellphone near the television causes the fluctuations in video or audio quality of television is one of the examples of EMI. EMI may lead to the adverse effect on the functioning of the important electronic systems/devices in the field of aerospace, defence, intelligence department, significant scientific research and also on human health due to prolonged radiation exposure [69–71]. The term EMI Shielding is referred to as the protection against the interruption of electromagnetic waves. The conductive material possesses good EMI shielding capability thus generally, the metal-based materials are used as EMI shield material but their weight to shielding effect ratio is more. Therefore nowadays, polymer-based conductive materials replaced them owing to their less weight, corrosion resistance, ease of processing, flexibility, and cost [69, 70, 72].

There are two kinds of conductive polymers; intrinsic conductive polymers (ICP) which have good electrical conductivity and extrinsic conductive polymers (ECP) in which electrical conductivity has to generate i.e. by conductive coating or conductive filler addition. There is a large range of conductive fillers are available categorized as; carbon-based and metal-based. Carbon-based fillers comprise as; CNT, CNF, CB, graphene, GR, GO, GNRs, GNPs, etc. And metals based metal nanowires, metal granules metal nanoflakes, etc. [69, 70].

The various structures were reported to enhance the absorption of electromagnetic waves as, segregated structure,

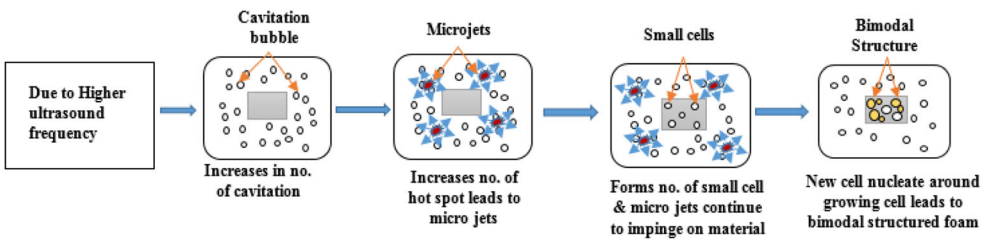

Fig. 12 Schematic representation of the formation of bi-modal ABS foam structure using ultrasound excitation

Table 4 Literature review on bi-modal microcellular foaming (Two-step depressurization)

Author	Material	Process Parameter	Findings	Ref
Bao et al.	PS	P_1 = 20 MPa, T_1 = 100 °C, t_1 = 4 h, P_2 = 15 MPa, t_2 = 0,10,30,45,60 min	Degree of depressurization and holding time significantly controlled density of large cells and small cells.	[43]
Bao et al.	PS	P_1 = 20 MPa, T_1 = 100 °C, t_1 = 4 h, P_2 = 12,13,15,17 MPa, t_2 = 0,10,30,45,60 min	Tensile and impact strength of bi-modal foam varies with volume fraction of large cell.	[44]
Z. Ma et al.	PC	P_1 = 20 MPa, T_1 = 60 °C, t_1 = 6 h, P_2 = 14 MPa, t_2 = 1 h,T_2 = 60 °C	Tensile strength & modulus improved by 28% & 32% respt. For foam having bi-modal structure compared to uni-modal structure due to blunting effect.	[45]
Z. Ma et al.	PC	P_1 = 20 MPa, T_1 = 60 °C, t_1 = 6 h, P_2 = 14 MPa, t_2 = 1 h,T_2 = 60 °C	Dielectric properties of the bi-modal structure were similar to a uni-modal structure as it depends on the porosity of foam.	[46]
P. Yu et al.	PLA/PBS blends	P_1 = 20 MPa, T_1 = 150 °C, t_1 = 1 h, P_2 = 16 MPa, t_2 = 10 min, T_2 = 90,100,110 °C	PLA/PBS blend in 80/20 ratio at 100 °C has highest cell opening rate of 96%	[47]
Wang et al.	PS/PETG blend	P_1 = 20 MPa, t_1 = 4 h, P_2 = 17.5 MPa	Bi-modal structure has a large-cell of diameter is 300 μm or more and small-cell of diameter is 100 μm or less.	[48]
C. Li et al.	PS	P_1 = 16 MPa, T_1 = 100 °C, t_1 = 2 h, P_2 = 12 MPa,T_2 = 100 °C	Density of larger cell & small cell governs by first degree of depressurization & second degree of depressurization respect.	[49]
Chen et al.	PCL	P_1 = 20 MPa, T_1 = 40 °C, t_1 = 2 h, P_2 = 12,10,8,7,6,5 MPa, t_2 = 1 h	Bi-modal porous scaffolds fabricated with a large cell size of 100 μm and smaller with 50 μm.	[50]
Arora et al.	PS	P_1 = 6000 psi, T_1 = 100 °C, hr., P_2 = 4000 psi, t_2 = 1 h	Bi-modal foam with an average cell size of the large cells and small cells about 21 μm and 4.8 μm fabricated.	[51]
Bernardo et al.	PMMA, PMMA/ MAM, PMMA/ SEP	P_{1PMMA} = 31 MPa, $P_{1PMMA/MAM}$ = 10 MPa, $P_{1PMMA/SEP}$ = 10 MPa, T_1 = 25 °C, t_1 = 24 h, P_{drPMMA} = 100 MPa/s, $P_{drPMMA/MAM}$ = 15 MPa/s, $P_{drPMMA/SEP}$ = 15 MPa/s, t_2 = 1 to 1.5 min	Proposed a model to predict thermal conductivity with consideration of bi-modal structure which provide more accurate estimation than model with mono-modal structure.	[62]
Gandhi et al.	ABS	P_1 = 5, 4, 3 MPa, T_1 = R.T, t_1 = 24 h, P_2 = 3, 2, 1.5, 1 MPa, T_2 = 100, 110, 120, 130, 140 °C	In bi-modal structure, size of primary bubbles and secondary bubbles influence by initial saturation pressure and holding time & holding pressure respect.	[63]

multilayer structure, sandwich structure and foam structure [71]. The density of polymer composite is less than metal composite but due to the addition of conductive filler, the density and the viscosity of polymer composite may increase. The researchers strive to further reduce the density of polymer composites by developing a porous structure in the polymer matrix [69, 71]. The reflection, absorption, multiple-reflection, and transmission are the mechanisms that play a significant role in locking the electromagnetic waves in the shielding material [69]. EMI shielding effectiveness (EMI SE) is a measure of the shielding material's performance, which is the sum of losses associated with all the above mechanisms and given in terms of decibel (dB) [69, 70, 72, 73]. In this study, this section is focussed on EMI shielding of the foam structure. The multiple-reflection mechanism occurs in foamed EMI shielding material because the foamed EMI shielding material has a large interface area and surface area so multiple-reflection possible [69].

Yang et al. [74] integrated hot pressure compression moulding and salt leaching process to develop PS/CNT foamed composite having a density of 0.45 and 0.27 g/cc.

Ling et al. [75] used the water vapour induced phase separation (WVIPS) process shown in Fig. 14 to produce microcellular nanocomposite foams for enhancement of EMI

Table 5 Literature review on bi-modal microcellular foaming (Co-blowing agent)

Author	Material	Blowing agent	Foaming process	Findings	Ref
Lee et al.	PS	Primary- n-butane Co- Water Nucleating agent- Silica particles	Extrusion foaming	Bi-modal structure can be tuned with the variation in co-blowing agent content. With an increase in water content enhanced the expansion ratio.	[40]
Zhang et al.	PS	Primary- CO_2, Co- Water Additives- GR, AC, CNF	Extrusion foaming	Foaming of PS with 0.5% GR & 0.5% AC with 0.5% water produced bi-modal Structure	[52]
Zhang et al.	PS	Primary- CO_2 Co- Water Additives- GR, AC, Nano Clay 30B	Extrusion foaming	Addition of particulates reduced the difference in foaming time. In PS/GR and PS/AC/GR both show bi-modal structure, in that PS/GR has small cells than PS/AC/GR.	[42]
Nistor et al.	PS	Primary- CO_2 nC5 & cC5	Batch foaming	Organic agents were used to enhanced foam porosity	[53]
Daigneult & Gendron	PS	Blend of CO_2 & 2-EH	Extrusion foaming	At 8.6 wt% of CO_2 & 1.6 wt% of 2- EH bi-modal cell size distribution was observed with a large cell size of about 250 μm and a small-cell size of about 25 μm.	[54]
Dugad et al.	ABS	Primary- CO_2 Co- Water	Batch foaming	Cell size enhanced with introduction of water which enhanced the expansion ratio	[64]

Shielding. Figure 15 depicts microwave transfer across nano-composite foam that enables composite foam as an excellent microwave absorber. Table 8 represents the literature review on EMI shielding microcellular polymers.

Auxetic foamed polymers

The auxetic polymers are processed materials having negative Poisson's ratio (NPR) by the virtue of which it explores the exceptional properties [89–92]. The material with NPR indicates, the material expands laterally when stretched linearly and vice versa [93–95]. The first polymer auxetic foam was synthesized by Lakes R. in 1987, had Poisson's ratio of −0.7 and Young's Modulus of 72 kPa from open-celled PS foam [89]. The auxetic foam has superior properties over conventional as; resilience, synclastic, indentation resistance, shear resistance, etc. which leads to the wide range applications in the field of aerospace, military, sports, biomedical, etc. [89, 90, 92, 96–99].

Generally, the thermo-mechanical technique is used for the transformation of conventional polymer foam to auxetic polymer foam. The thermo-mechanical technique is comprised of three steps; first is volumetric compression of conventional foam using a mould of which shape is to be achieved. In this step, the buckling of cell ribs or struts occurs which leads to a re-entrant cell structure. Then second is a heating step, in which compressed foam along with mould heated in a furnace at a temperature above the softening temperature to maintain the buckled cell structure for a defined time. Finally in third step, mould takes out from the furnace, cooled it to room temperature and

Table 6 Literature review on bi-modal microcellular foaming (Polymer blend technique)

Author	Blend Composition	Foaming Process	Process Condition	Findings	Ref
Kohlhoff et al.	PMMA & PS	Batch foaming	$P_1 = 8$ MPa, $T_1 = 60$ °C, $t_1 = 4$ h, $T_2 = 100$ °C P2 = 8 MPa, $t_2 = 4$ h	Bi-modal cell structure with diameter range for small cells 10–30 μm and for large cell 200–400 μm were observed in blend ratio of 50:50, 33:67, 15:85	[57]
Lei Jiang et al.	PP/LDPE	Batch foaming	$P_1 = 25$ MPa, $T_f = 100$ °C, 90 °C, & 140 °C,150 °C $R_{dp} = 400$ MPa/s	Bi-modal structure generated in pure PP, 90:10 & 75:25 PP: LDPE Blend foam.	[55]
Tang et al.	PP and PP/PLA & talc	Batch foaming	$T_f = 82$ °C to 99 °C.	Bi-modal structure was observed at a low temperature of 93 °C & 94.5 °C in PP foam. And in PP/PLA blend foam at 90 °C.	[56]
Wang et al.	PP/ PS blend and clay	Tandem extrusion foaming	First barrel pressure = 7 bar & second barrel pressure = 10.5–18 bar	Bi-modal structure was observed in PP/PS blend in the ratio of 80/20, 70/30, 60/40. Large cell Density increases with an increase in PS concentration.	[58]

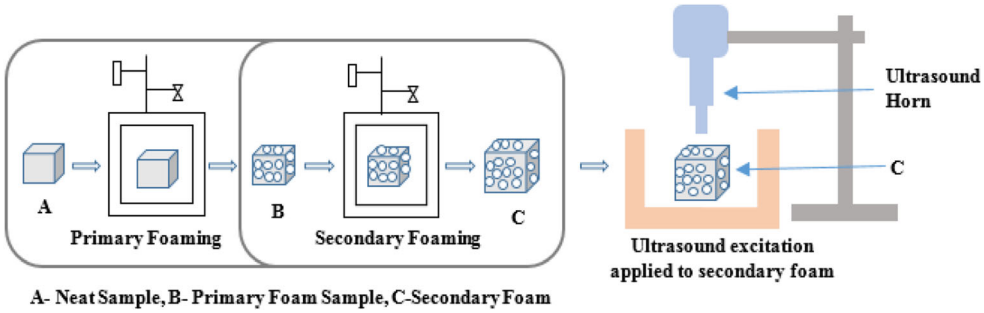

Fig. 13 Schematic representation of ultrasound-induced cyclic foaming process- adapted from Ref [38] with kind permission from Elsevier

remove the foam from it. Sometimes cell ribs stick to each other which may affect the functionality of final foam (auxetic) thus stretch the foamed sample in the opposite direction of compression [89, 100–103]. It is recommended to lubricate inside the mould or use of wire or tweezers or redesign the mould to avoid the surface wrinkling or surface creasing [97].

To eliminate the high temperature processing, Garima et al. [104] developed a novel chemo-mechanical technique. In this technique, the first compression step was similar to as in thermo-mechanical technique. Then compressed foam sample wrapped in filter paper and placed in the organic solvent (acetone) for a defined time. Finally taken out the sample and dried it in the air. The formed foam was auxetic in nature. Also, the researchers successfully re-convert auxetic foamed structure to the original foamed structure using the same organic solvent through the re-expansion of the auxetic foamed sample in the solvent.

The simple geometry auxetic foams are easy to manufacture than complex and curved geometry auxetic foams using above mentioned conventional techniques. As the solution for this, Binachi et al. [105] developed a new method called half mould manufacturing process. In this method, the author used an open curved mould instead of a closed mould. The conventional foamed sample placed in mould on which layer of non-porous fluorinated ethylene propylene (FEP) film and over that the medium weighs polyester nonwoven breather blanket placed such a that it covers foamed sample with mould. The assembly closed in the flexible membrane and sealed it properly then using a vacuum pump reduced internal pressure to 0.7 Bar. Due to vacuum, cell ribs get bucked and re-entrant structure was formed. To preserve the cell structure, all assembly was kept in a furnace of temperature 200 °C by maintaining inside vacuum. After a definite heating time of half-hour, assembly was taken out and immersed in water. Once the temperature reached to room temperature foamed sample outstretched orthogonally to relive cell sticking. The resultant foam was in auxetic nature.

The transformation of closed cell conventional foam to auxetic foam is difficult than open cell conventional foam to auxetic foam which may be due to isolated cell or thick cell walls. Fan et al. [106] proposed a new technique using water steam called steam penetration and condensation (SPC). In this technique, the foamed sample of defined shaped placed in water steam environment which maintains at a specific temperature for a defined time. Due to steam, all cells contracted inside leads to cell bucking, re-entrant structure.

Table 7 Literature review on cyclic microcellular foaming

Author	Material	Foaming process	Findings	Ref.
Gandhi et. al	ABS	Batch foaming	Developed 0.02 g/cc low density foam with the cell size enhancement using cyclic foaming.	[38]
Seo et al.	PC	Batch foaming	If $P_1 > P_2$ then cell density increased & if $P_2 > P_1$ cell size enhanced.	[66]
Cho et al.	PC	Batch foaming	P_1 significantly affects cell morphology than P_2. Also, the sequence of processing affects both cell morphology and foaming ratio.	[65]
Nawaby &. Handa	PMMA	Batch foaming	The foam density of secondary foam significantly reduced up to 6 days aging after that plateau occurs. Also the density of secondary foam with N_2 nearly the same to primary foam.	[67]
Radhakrishna et. al	PMMA	Batch foaming	Cell buckling phenomenon was observed which resulted in star-like microstructure and low-density PMMA foam developed using cyclic foaming.	[68]

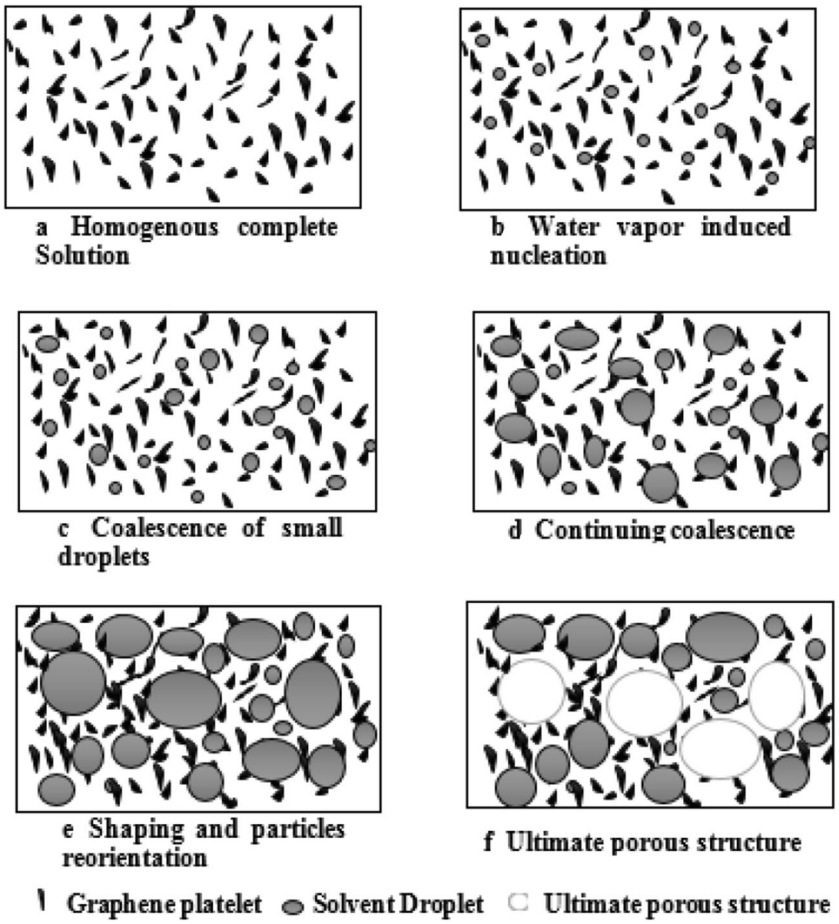

Fig. 14 Schematic representation of WVIPS process to prepare nanocomposite foam- adapted from Ref [75] with kind permission from American Chemical Society

Then the sample was taken out and cooled to room temperature. The foam structure resulting from this technique has NPR i.e. showing uniform auxetic nature due to the pressure difference.

In order to enhance the mechanical performance of auxetic foam compared to the performance of auxetic foam produced from the thermo-mechanical technique, the new technique was developed by Quadrini et al.

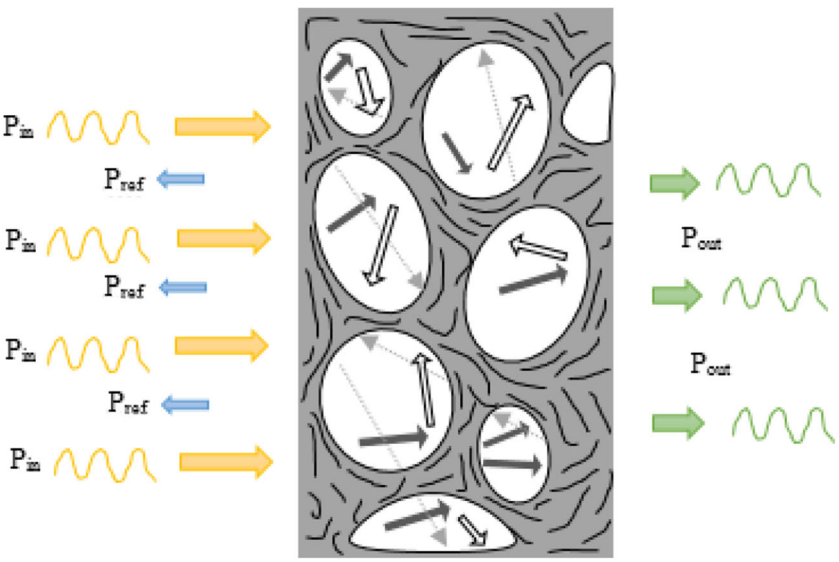

Fig. 15 Schematic representation of the microwave transfer across nanocomposite foam- adapted from Ref [75] with kind permission from American Chemical Society

Table 8 Literature review on EMI Shielding microcellular polymers

Author	Filler	Material	Composite preparation technique	Foaming process	Finding	Ref
Thomassin et al	MWCNT	PMMA	Precipitation polymerization Melt-blending, Co-precipitation	Batch-foaming	Compared to neat polymer sample foamed sample absorbed more than 90% of incoming power	[76]
X-B Xu et al.	CNT	PU	Static casting	Polymerization between polyol and isocyanate	Lightest PU/CNT composite with 0.05 g/cc fabricated.	[77]
Wang et al.	Graphite	PLA	Twin Screw extruder	Mould opening foam injection molding	PLA/graphene nanocomposite foam exhibits EMI SE upto 45 dB (i.e 99% radiation blocked)	[78]
Yang et al.	MWCNT	PS	Surfactant with ultrasonication	–	Foam composite with 7% CNT generated EMI SE about 20 dB	[79]
L Xu et al.	CNT	HDPE	Solution mixing & mechanical pulverization	Compression molding plus salt-leaching	Specific EMI SE of CNT/HDPE foam composite about 2.2 times of solid composite	[74]
D-X Yan et al.	FGS	PS	Solution mixing & mechanical pulverization	Compression molding plus salt-leaching	Porous, low-density FGS/PS composite foam exhibited EMI SE of 29 dB.	[80]
Zhang et al.	GS	PMMA	Solution Blending & melt compounding	Batch foaming	PMMA/ graphene composite foam with 1.8 vol% graphene shows an EMI SE of 13–19 dB	[81]
Shen et al.	G@Fe3O4 Hybrid	PEI	Solution Blending	WVIPS	Composite foam showed EMI SE of ~14.3–18.2 dB at a frequency range of 8–12 GHz	[82]
Shen et al.	GO	PU Sponge	–	Dip coating	PU/Graphene foam fabricated with a density range of 0.027–0.03 g/cc	[83]
Ling et al.	GNC	PEI	Solution Blending	WVIPS	Microcellular PEI/graphene foams at 7 & 10 wt% exhibits EMI SE of 36.1 & 44.1 dB/ (g/cm3) respect.	[75]
Zeng et al.	MWCNT	WPU	–	Freeze drying	Porous, anistropic MWCNT/WPU foam exhibits SE above 20 dB	[84]
Ameli et al.	CF	PP	–	Injection molding machine MuCell technology	PP/CF composite density reduced by 25% & EMI SE increased to 65%	[85]
Bernal et al	MWCNT, f- MWCNT & FGS	PU	Ultrasound-assisted the dispersion of (polyol & filler)	Open cylinder moluding	FGS/PU composite exhibited EMI SE of 15.15 dB cc/g. And for MWCNT & f-MWCNT it showed nearly the same	[86]
Ameli et al.	SSF	PP	–	Injection molding machine MuCell technology	PP/SSF composites showed EMI SE of 75 dB·g − 1 at 1.1 vol% SSF	[87]
Yu Xu et al.	MWCNT	Melamine foam	Solution blending and then ground in cone mill	Electroless silver plating	Epoxy composite with multiple conductive showed SE of 88 dB.	[88]

[107] called solid-state foaming for auxetic foam. In this method, first the epoxy resin powder tablets of re-entrant hexagonal shape were prepared by cold compaction. Here the number of small tablets were arranged in an ordered manner with defined space between them because the large size tablet leads to poor foaming. After that foaming of tablets was done using the oven at 320 °C for 8 min in the presence of air. Then the foamed samples were taken out and cooled in the air which showed auxetic behaviour.

For the manufacturing of large auxetic foam blocks, Chan et al. [108] proposed a multi-stage thermo-mechanical technique in which volumetric compression and heating occurred in stages. The advantage of this multi-stage method is that the surface ceasing is eliminated. Table 9 shows the literature review on auxetic foamed polymer.

Porous microcellular polymers

The large surface area, interconnected cell structure, small and uniform cell size increased demand of the porous microcellular polymer preferably for tissue engineering scaffolds, separation membranes, cushioning, etc. The scaffolds used for the transformation of nutrients, the excretion of cell wastes, cell interaction, tissue formation which required porous structure [109, 110]. The various techniques used for the fabrication of porous structure for scaffold as; solvent casting/particulate leaching, thermally induced phase separation, freeze-drying, etc. [110, 111]. These are conventional solvent-based techniques which may affect the ability of the biological cell to generate new cells [31], less pore-interconnectivity, uneven pore distribution, less porosity, etc. [109]. These problems are resolved by the gas foaming technique as it is a solvent-free technique [109, 110, 112].

Table 9 Literature review on Auxetic foamed polymers

Author	Material	Foaming process	Findings	Ref.
Lakes	Low-density PS-Open cell polymer foam	Thermo-mechanical	Successfully synthesized man-made auxetic foam with poison's ratio of −0.7 with properties like synclastic, high shear modulus.	[89]
Fan et al.	PE –Closed Cell foam	SPC	Auxetic foam with SPC successfully prepared and conclude that pressure difference due to steam condensation main reason for conversion of auxetic structure.	[106]
Grima et al.	PU foam – Open cell (30 pores per inch) foam	Chemo-mechanical	Auxetic foam with poison's ratio ranges from −0.32 to −0.36 obtained with new technique compare to thermo-mechanical technique it is more.	[104]
Bianchi et al.	PU foam – Open cell foam	Vacuum based assembly system	With novel technique curved auxetic foam with poison's ratio of −1.26 & -0.96 in yx and xy direction respectively at 5% tensile strain manufactured.	[105]
Bianchi et al.	PU-PE - Open cell foam	Thermo-mechanical	It reported that the foam density depends on the time delay to remove from the mould. More time delay leads to higher density.	[100]
Chan & Evans	Polyether urethane- open cell foam	Multi stage-thermo-mechanical	Poison's ratio can be controlled by the volumetric compression. The heating time, temperature and compression load required more for large sample compared with the small one.	[108]
Quadrini et al.	Commercial Epoxy Resin- powder	Solid-State foaming	New solid-state foaming without any additives directly results in foam with auxetic structure.	[107]
Wang & Lakes	PU- open cell foam	Thermo-mechanical	The study suggests that with auxetic effect reduces with a decrease in cell size. As poison's ratio of −0.8, −0.5, −0.4 for cell size of 20, 65,100 ppi respectively obtained at optimal heating temperature and time.	[101]
Yao et al.	PU foam as matrix & shape memory epoxy resin as functional phase	Thermo-mechanical	The auxetic effects enhance with the rise in the volume compression ratio. At a compression ratio of 0.79 maximum Poisson ratio (−0.43 ± 0.05) obtained.	[102]
Alderson et al.	PU- open cell foam	Thermo-mechanical Uniaxial compression within a specially designed rig	For the curved foams and flat sheets, Poisson's ratio values reported as −3 and − 0.3.	[103]

Presently, advanced techniques such as electrospinning and 3D printing or rapid prototyping are using to achieve better specific structure properties with ease of processing at economical cost. Electrospinning is used to fabricate a porous scaffold using fibers, it's a simple and cost-effective fiber production technique. In this technique, the high voltage supply applied to polymer droplet held at tip of needle, which charges the droplet & formed repulsive force. The charged jet of polymer solution erupts and reaches to a collector, solvent evaporates and jet solidified into thin fibers [111, 113–115]. Another technique called, 3D printing or rapid prototyping technique is used to fabricate complex scaffold structures precisely from biodegradable materials [110, 116–121]. Also, some researchers modified or integrated two or more techniques to achieve the advance structure [122–126]. This section focused on porous microcellular plastics using a gas foaming technique.

To fabricate the porous or open interconnected structure, the ultrasound assistance was also used by various researchers such as Gandhi et al. [38], Wang et al. [31], H Wang et al. [34], X Wang et al. [36] for different applications. Table 10 contains the literature review on porous microcellular plastic.

Wood fiber reinforced microcellular polymer composites

Wood fillers or flour as reinforcement in polymer matrix led to the new branch of composites termed as wood fiber reinforced polymer composite (WFRP). At present, WFRP composites are the most demandable composites in different fields like construction for interior decoration & furniture, automotive for decking, window, and door lineals, railing, auto parts, etc. due to its mechanical properties [135–139]. The WFRP composites are generally manufactured by injection moulding, extrusion and compression moulding [135, 137]. The reason behind the huge demand of WFRP composite is, readily available wood filler at low cost, has specific strength and biodegradability [135–137]. The various wood fillers, with different aspect ratio are available in the form of fiber or flour [137]. There are some constraints for the utilization of wood fibers such as; thermal degradation, fiber breakage, and moisture content which limits the selection of processing parameters [135, 137, 140]. The WFRP composites possess good strength and stiffness so it could be utilized for static applications but also has low impact strength, brittleness, and high bulk density which limits its utilization in dynamic applications [140–143]. Therefore to advance its utilization in dynamic applications, the mechanical properties have to be enhanced (impact strength & ductility has to enhance with a reduction in bulk density), which could be achieved by the creation of microcellular structure in composites [136, 141, 144, 145].

The microcellular structure could be generated in wood composites by foaming processes such as; batch foaming, injection mould foaming, extrusion foaming, compound Moulding [136, 141, 145]. Some advancement is still going on to develop a new process or modify the existing ones as; co-extrusion, foaming during extrusion, and inline coating technologies, etc. [138]. The advantages of foamed wood composite over the unfoamed wood composite are low processing temperature, high production speed which in turn reduced manufacturing cost also better surface smoothness, sharp counters, and corners, etc. [136, 144, 146].

The process of WFRP composite foaming is similar to the general foaming process comprised of three stages; gas dissolution & saturation, cell nucleation, and cell growth & stabilization. In wood-composite foaming, blowing agent is not dissolved in wood fillers thus only polymer matrix gets plasticized. Subsequently, due to the generation of thermodynamic instability, cell nucleation occurs. In this case, both types of nucleation occur; homogenous as well as heterogeneous. The homogenous nucleation due to the gas diffusion from the composite whereas heterogeneous nucleation due to the entrapped gas at micro-voids near polymer-filler interfaces. The percentage of heterogeneous nucleation is more than the homogenous nucleation because of the more filler content, the number of interfaces available and restricted the gas dissolution to the polymer matrix. The continue cell growth may lead to cell coalescence and cell collapse, [136, 141]. To avoid this, the cells are stabilized using a cooling medium.

A wide variety of additives are used to form wood composites such as coupling agents to improve the dispersion of fillers, chemical surfactants to enhance the bonding or adhesion between filler and polymer matrix, flame retardants to enhance resistance to the outbreak of fire, etc. [139–141, 144, 145, 147–150].

Some researchers fabricated wood composites from the wastes; PS foam as polymer matrix and agricultural waste as a wood filler. Koay et al. [151] prepared novel wood composite from recycled PS foam and durian husk fiber. In this, first PS foam sample was dissolved in acetone to remove air from it. Later it was dried at 70 °C using oven followed by filtration; subsequently recycled PS was cut into small samples for further process. For wood fiber, durian husks were collected, cleaned and cut into small pieces then dried it in an oven at the same 70 °C and prepared short fiber with the grinder. The fibers dried again to avoid high moisture content. Subsequently, WPC compound formed using torque rheomix and moulded into sheets using hot press. Similarly, Tawfik et al. [152] formed a wood composite with recycled PS and rice straw. The tensile strength, water absorption, and acoustic resistance test were performed. The tensile strength decreased with an increase in rice straw content above 30%. Chun et al. [153] used agricultural waste to formed wood composite with PS foam. The tensile, thermal and morphological evaluation

Table 10 Literature review on Porous microcellular polymers

Author	Material	Process	Findings	Ref
Mancuso et al.	AW & two silicate-based novel glasses	Binder jetting 3D printing and sintering	Structure with the accuracy of ±0.25 mm created	[119]
Seleznev et al.	PLA	Combination of 2D nano imprint & 3D printing (SLA)	Polymer bone scaffold fabricated with a hybrid technique	[118]
Mohanty et al.	PVA	Combined 3D printing and salt leaching	Double pore scaffold with uniform cell distribution, high cell density fabricated with a combined technique	[117]
Jakus et al.	Graphene & PLGA	3D printing	Graphene-based scaffold fabricated with filaments of diameter ranges from 100 to 1000 μm	[120]
Zein et al.	PCL	Fused deposition modelling (FDM)	PCL scaffold with the porosity of 48–77%, range of yield strength 0.4–3.6 MPa & strain yield 4% -28%	[121]
Huang et al.	PLA	Electrospinning	Electrospin fibers with 100 nm sized pores fabricated using chloroform solvent as a volatile solvent	[113]
Qin et al.	5 wt% PLA dissolved in DMF/ CH_2Cl_2	Electrospinning	Durable, uniform, flexible white-light-emitting fibrous membrane fabricated with coaxial electrospinning	[114]
T Xu et al.	PCL, cellulose acetate	Electrospinning	Interconnect structure scaffold with the porosity about 95% & pore size from submicron to 100 μm fabricated	[115]
Jaganathan et al.	PU, Corn oil, Neem oil, DMF	Electrospinning	Addition of corn oil & corn/neem oil reduced fiber diameter from 890 ± 116.911 nm to 845 ± 117.86 nm & 735 ± 126.49 nm respt.	[127]
Thakare et al.	PCL, ZrO_2	Electrospinning	Scaffold with ZrO_2 enhanced the cell adhesion and proliferation.	[128]
Wang et al.	PCL, CBA- SB, PBA- CO_2	Chemical injection mould foaming combined with particulate leaching	Scaffolds with porosities of 68.2%, 73.8%, and 70.9% for different samples; A, B, and C respect. Fabricated	[122]
Kramschuster et al.	PLA, PVOH, Particulate- NaCl, PBA- CO_2	Physical injection molding combined with particulate leaching	Interconnected pores structure about 200 μm in diameter and porosities of about 75% fabricated.	[120]
Huang et al.	PCL, PEO, PBA- N_2	Combined injection mould foaming and polymer leaching	Blend of PCL/PEO (50%/50%) enhanced porosity to 89.5% & compression modulus decrease to 46.7 MPa from 68.2 MPa	[124]
Matuana et al.	PLA, PBA- CO_2, NA-Montmorillonite clay, quaternary bis (2-hydroxy ethyl) ammonium salt	Continuous-extrusion foaming	Higher porosity obtained by high gas flow rate and high-pressure drop	[129]
Gomes et al.	Starch, PBA- CO_2	Extrusion foaming, compression moulding & particle leaching, and solvent casting & particle leaching	Higher porosity about 60–70% reported with solvent casting & particle leaching	[130]
Jing et al.	PCL & CSNF	Combined extrusion foaming, water-soluble phase leaching, and freeze-drying.	Compressive modulus & water uptake capacity of scaffold enhance by 35% with utilization CSNF	[125]
Gandhi et al.	LDPE, CBA- N_2	Extrusion foaming process by rapid surface quenching technique	High blowing agent content induced open cell structure and at lower chill roll speed & temperature open cell with interconnected structure was observed	[126]
Sierraa et al.	PCL, PBA- CO_2, THF, & EtOAc	$ScCO_2$ foaming	Membrane with the larger pore of 300–500 μm surrounded by smaller pore of 15–50 μm prepared	[131]
Cue'noud et al.	Blend of PLLA, PLDLA, PEG flakes	Batch foaming	Open-cell structure with cell dia. 200 μm −700 μm & porosity more than 75% generated	[132]
Floren et al	PDLLA	Batch foaming	Mechanical anisotropy and performance of foamed specimen depends on processing parameters	[133]
Singh et al.	PLGA	Batch foaming	Interconnected structure with 89% porosity and pore size ranges from 30 to 100 μm generated	[134]

Table 11 Literature review on wood fibre reinforced microcellular polymer composite

Author	Material	Filler and additives	Mixture process	Foaming process	Finding	Ref
Rachtanapun et al.	Blend of HDPE/PP	Wood fiber	Twin-screw extruder	Batch foaming	Gas solubility and void fraction decrease due to high filler crystallinity and increased stiffness.	[154]
Fatih M. et al	PVC	Wood flour, and CBA- azodicarbon-amide & SB	High-intensity Mixer	Extrusion foaming	CBA content and type has no effect on the density reduction of the foamed composite.	[155]
Zhang et al.	PP	Wood fiber, Flame retardants- APP & silica	Twin-screw extruder	Batch foaming	Smaller cell size and high relative density in case of silica and in APP density first decreases and then increase with enhanced cell size	[139]
Zhang et al.	PP	Wood Flour, CA- MAPP CBA-Foamazol R71 Antioxidant & stabilizer- Irganox B215	Twin-screw extruder	Extrusion foaming	Composite foam with average cell size less than 100 μm obtained and coupling agent enhance bonding between PP & wood flour.	[140]
Bledzki et al.	PP	Hardwood fiber, CA- MAPP, CBA- Hydrocerol 530, Hydrocerol AB40E, Hydrocerol BIH20	High-speed mixer	Injection moulding	Nearly 70% of surface roughness decreases using an endothermic foaming agent and physico-mechanical properties enhanced up to 80%.	[144]
Zhang et al.	PP	Wood Fiber, compatibilizers- SEBS-g-MA, PP-g-MA, Silica (aerogel 150)	Twin-screw extruder	Batch-foaming	Cell Density increases and cell size decreases with silica content due to heterogeneous nucleation	[150]
Q Li et al.	HDPE	Wood flour, CBA- SB, Celogen-OT, Celogen-AZNP & EX210, CA- MA-g-HDPE	High-intensity mixer	Extrusion foaming	Void fraction depends on CBA content than CBA type. (1% for neat HDPE and 0.5% for HDPE/wood-flour composites	[142]
B Xie et al.	Recycled PP	Wood Fiber, CBA- azodicarbonamide, CA- MAPP	Single-screw extruder	Injection molding	Density reduction by 24.5% and impact strength enhancement by 53% of the composite.	[145]
Lee et al.	HDPE	Wood Fiber, CA- MA-g-HDPE, Nano clay- Cloisite 20A (intercalated and exfoliated)	Masterbatch and direct melt blending	Extrusion foaming	At low wood fiber content 1% clay significantly affects cell morphology.	[143]
Choe et al.	PU	Chemically treated wood fiber, CS- NaOH & γ-aminopropyltriethoxysilane	Stirred Mixer	One-shot polymerization	Chemical treatment enhanced the open porosity which increases sound absorption	[147]
Feng et al.	PVC	Wood Fiber CS- NaOH & 3-triethxysilyl-1-propanamine (KH-550)	Tank-ball mill mixed	One-step compression moulding	Compared to both chemical surfactants NaOH treated gave the best result. The tensile strength more for small particle-sized wood fiber composite.	[148]
Yeh et al.	PP	Rice husk, CA- SEBS-g-MA & PP-g-MA, CS- NaOH, silane, NaOH + HCl + silane	Brabender plasticorder (PLE-331) internal mixer	Batch foaming	Fiber surface treatment and coupling agent significantly enhance the cell morphology and reduce the density.	[149]
Khoshnoud & Abu-Zahra	PVC	Mica, glass fiber, and fly ash	High shear mixer	Extrusion foaming	The glass fiber composite has better flexural and impact strength than mica and fly ash composite.	[156]

was done to analyze the performance of composites. Table 11 represents the literature review on wood fiber reinforced microcellular polymer composite.

Conclusions and future direction

- The manufacturing of customized polymer foam with controlled cell morphology using general microcellular foaming is quite difficult. Therefore, the integration of advancement to traditional methods has been made more convenient and effective.
- The advancement in the microcellular foaming process such as ultrasonication has been found to be much effective in enhancing both nucleation rate as well as interconnected open-cell structure. It depends on the time of application of the ultrasonication (i.e. at the beginning of nucleation or after nucleation)
- The microcellular polymer composites exhibit a better EMI Shielding effect than neat polymer composites with a reduction in weight density too.
- Carbon-based fillers are the most suitable fillers to enhance the electrical conductivity of polymer foam in EMI shielding applications due to their wide range of properties.
- In wood fiber reinforced polymer foaming, the cell nucleates by homogenous nucleation as well as heterogeneous nucleation. Homogenous nucleation occurs due to gas diffusion from polymer matrix whereas, heterogeneous nucleation takes place at polymer-filler interface due to entrapped gas at micro-voids.
- The buckling of cells governs the auxetic behaviour and the performance of auxetic foam polymer is independent of the cell size of the foam structure.
- The bi-modal cell structure provides superior properties compared to the uni-modal cell structure. Moreover, the tri-modal cell structure may add more value to properties governed by the bi-modal structure. Hence, there is scope to further develop the polymeric foam with tri-modal or multi-modal cell structure.
- Few literatures are available on the cyclic foam manufacturing process which builds up research focus to explore more and more on the cyclic foaming technique to manufacture ultralow density foam with desired properties.

Acknowledgements Financial assistance has been received from the Department of Science and Technology (DST), Government of India under the project titled "Development of Microcellular & Nanocellular 3D Printing Process to Manufacturing Acrylonitrile Butadiene Styrene Foamed Products".

Grant order: DST/TDT/AMT/2017/092 (G).

Abbreviations *CBA,* Chemical blowing agent; *PBA,* Physical blowing agent; *CA,* Coupling agent; *NA,* Nucleating agent; *CS,* Chemical surfactants; CO_2, Carbon dioxide; $ScCO_2$–, Supercritical CO_2; N_2, Nitrogen; *ABS,* Acrylonitrile-Butadiene-Styrene; *PS,* Polystyrene; *PE,* Polyethylene; *PC,* Polycarbonate; *PP,* Polypropylene; *PMMA,* Polymethyl methacrylate; *LDPE,* Low-Density Polyethylene; *HDPE,* High-Density Polyethylene; *PVOH,* Polyvinyl alcohol; *PEG,* Polyethylene glycol; *PLA,* Poly (lactic acid); *PLLA,* Poly-L-lactide; *PLDLA,* Poly-L-lactide-co-D, L-lactide; *PDLLA,* Poly (D, L lactic acid); *PVC,* Poly (vinyl chloride); *PLGA,* Polylactide-co-glycolide; *PVOH,* Polyvinyl alcohol; *PEO,* Poly (ethylene oxide); *PBS,* Poly (butylenes succinate); *PETG,* Poly (ethylene terephthalate glycol); *PCL,* Poly (ε-caprolactone); *PVA,* Polyvinyl alcohol; *PVDF,* Polyvinylidene fluoride; *PEI,* Polyethyleneimine; *PANI,* Polyaniline; *MAM,* Poly (methyl methacrylate)-poly (butyl acrylate)-poly (methyl methacrylate); *PU,* Polyurethane; *WPU,* Water-borne polyurethane; *ZnS,* Zinc stearate; *SEP,* Sepiolites,; *nC5,* Co-n-pentane; *cC5,* Cyclopentane; *2-EH,* 2-ethyl hexanol; *AW,* Apatite–wollastonite; *DMF,* Dimethylformamide; *CSNF,* Chitosan nanofibers; *THF,* Tetrahydrofurane; *EtOAc,* Ethylacetate; *SEBS-g-MA,* Maleic anhydride- grafted styrene–ethylene–butylene–styrene; *PP-g-MA,* Maleic anhydride-grafted polypropylene; *APP,* Ammonium polyphosphate; *MAPP,* Maleated PP; *SB,* Sodium bicarbonate; *NaCl,* Sodium chloride; *HCL,* Hydrochloric Acid; *NaOH,* Sodium Hydroxide; *CB,* Carbon black; *AC,* Activated carbon; *CNT,* Carbon nanotubes; *CNF,* Carbon nanofibers; *GR,* Graphite; *GO,* Graphene oxide; *GNC,* Graphene Nano composite; *GNRs,* Graphene nanoribbons; *GNPs,* Graphene nanoplatelets; *GS,* Graphene sheets; *FGS,* Functionalized graphene sheets; *MWCNT,* Multi-wall carbon nanotube; *f-MWCNT,* Functionalized MWCNT; *SSF,* Stainless-steel fiber; ZrO_2, Zirconia

References

1. Okolieocha C, Raps D, Subramaniam K, Altstädt V (2015) Microcellular to nanocellular polymer foams: Progress (2004-2015) and future directions - A review. Eur Polym J 73:500–519
2. Li R, Zeng D, Liu Q, Li L, Fang T (2015) Physical properties of microcellular polymeric foams with supercritical CO 2. Mater Res Innov 19(sup5):S5–250–S5–256
3. Sorrentino L, Aurilia M, Iannace S (2011) Polymeric foams from high-performance thermoplastics. Adv Polym Technol 30(3):234–243
4. M Altan. Thermoplastic foams: Processing, manufacturing, and characterization. Polymerization. London: IntechOpen; 2018. 117–137 p
5. Xu Y, Zhang S, Peng X, Wang J (2018) Fabrication and mechanism of poly(butylene succinate) urethane ionomer microcellular foams with high thermal insulation and compressive feature. Eur Polym J 99:250–258
6. Prasad K, Nikzad M, Sbarski I. Permeability control in polymeric systems: a review. Vol. 25, Journal of Polymer Research. Springer Netherlands; 2018. p. 1–20
7. Zhang H. Scale-up of extrusion foaming process for manufacture of polystyrene foams using carbon dioxide. University of Toronto; 2010
8. Nofar M, Park CB. Introduction to plastic foams and their foaming. In: Polylactide Foams. Elsevier; 2018. p. 1–16
9. Jin FL, Zhao M, Park M, Park SJ (2019) Recent trends of foaming in polymer processing: A review. Polymers 11(6):953
10. Laguna-Gutierrez E, Escudero J, Kumar V, Rodriguez-Perez MA (2018) Microcellular foaming by using subcritical CO 2 of

crosslinked and non-crosslinked LDPE/clay nanocomposites. J Cell Plast 54(2):257–282
11. Shea JJ. Polymeric foams: mechanisms and materials [Book review]. Vol. 21, IEEE Electrical Insulation Magazine. CRC Press; 2005. 56–56 p
12. Pinto J, Reglero-Ruiz JA, Dumon M, Rodriguez-Perez MA (2014) Temperature influence and CO2 transport in foaming processes of poly(methyl methacrylate)–block copolymer nanocellular and microcellular foams. J Supercrit Fluids 94:198–205
13. Guanghong H, Yue W. Microcellular foam injection molding process. In: Some Critical Issues for Injection Molding. IntechOpen; 2012. 175–202
14. Yeh SK, Chen YR, Kang TW, Tseng TJ, Peng SP, Chu CC et al (2018) Different approaches for creating nanocellular TPU foams by supercritical CO2 foaming. J Polym Res 25(1):1–12
15. Lang X, Hua, Wang D, Prakashan K, Zhang X, Zhang ZX (2017) Microcellular chlorinated polyethylene (CM) rubber foam by using N2 as blowing agent. J Polym Res 24(11):1–11
16. Kumar V, Suh NP (1990) A process for making microcellular thermoplastic parts. Polym Eng Sci 30(20):1323–1329
17. Goel SK, Beckman EJ (1994) Generation of microcellular polymeric foams using supercritical carbon dioxide. I: effect of pressure and temperature on nucleation. Polym Eng Sci 34(14):1137–1147
18. Kumar V, Weller JE. Microcellular Foams. In: Polymeric Foam. 2009. 101–14
19. Bao D, Liao X, He T, Yang Q, Li G (2013) Preparation of nanocellular foams from polycarbonate/poly(lactic acid) blend by using supercritical carbon dioxide. J Polym Res 20(11):1–10
20. Singh I, Gandhi A, Biswal M, Mohanty S, Nayak SK (2018) Multi-stage recycling induced morphological transformations in solid-state microcellular foaming of polystyrene. Cell Polym 37(3):121–149
21. Shi X, Wang L, Kang Y, Qin J, Li J, Zhang H et al (2018) Effect of poly(butylenes succinate) on the microcellular foaming of polylactide using supercritical carbon dioxide. J Polym Res 25(11):1–12
22. Sauceau M, Fages J, Common A, Nikitine C, Rodier E (2011) New challenges in polymer foaming: A review of extrusion processes assisted by supercritical carbon dioxide. Prog Polym Sci 36(6):749–766
23. Di Maio E (2018) Foaming of polymers with supercritical fluids and perspectives on the current knowledge gaps and challenges. J Supercrit Fluids 134:157–166
24. Gandhi A, Bhatnagar N (2015) Physical blowing agent residence conditions stimulated morphological transformations in extrusion foaming. Polym-Plast Technol Eng 54(17):1812–1818
25. Nalawade SP, Picchioni F, Janssen LPBM (2006) Supercritical carbon dioxide as a green solvent for processing polymer melts: processing aspects and applications. Prog Polym Sci 31(1):19–43
26. Hou J, Zhao G, Wang G, Dong G, Xu J (2017) A novel gas-assisted microcellular injection molding method for preparing lightweight foams with superior surface appearance and enhanced mechanical performance. Mater Des 127:115–125
27. Tomasko DL, Burley A, Feng L, Yeh SK, Miyazono K, Nirmal-Kumar S, Kusaka I, Koelling K (2009) Development of CO2 for polymer foam applications. J Supercrit Fluids 47(3):493–499
28. Wang J, Zhai W, Ling J, Shen B, Zheng W, Park CB (2011) Ultrasonic irradiation enhanced cell nucleation in microcellular poly(lactic acid): A novel approach to reduce cell size distribution and increase foam expansion. Ind Eng Chem Res 50(24):13840–13847
29. Guo G, Ma Q, Zhao B, Zhang D (2013) Ultrasound-assisted permeability improvement and acoustic characterization for solid-state fabricated PLA foams. Ultrason Sonochem 20(1):137–143
30. Wang H, Li W (2008) Selective ultrasonic foaming of polymer for biomedical applications. J Manuf Sci Eng 130(2):021004
31. Wang X, Li W, Kumar V (2009) Creating open-celled solid-state foams using ultrasound. J Cell Plast 45(4):353–369
32. Niemczewski B (2007) Observations of water cavitation intensity under practical ultrasonic cleaning conditions. Ultrason Sonochem 14(1):13–18
33. Gandhi A, Asija N, Chauhan H, Bhatnagar N (2014) Ultrasound-induced nucleation in microcellular polymers. J Appl Polym Sci 131(18):9076–9080
34. Wang X, Li W, Kumar V (2006) A method for solvent-free fabrication of porous polymer using solid-state foaming and ultrasound for tissue engineering applications. Biomaterials. 27(9):1924–1929
35. Youn JR, Park H (1999) Bubble growth in reaction injection molded parts foamed by ultrasonic excitation. Polym Eng Sci 39(3):457–468
36. Zhai W, Yu J, He J (2008) Ultrasonic irradiation enhanced cell nucleation: an effective approach to microcellular foams of both high cell density and expansion ratio. Polymer. 49(10):2430–2434
37. Byon SK, Youn JR (1990) Ultrasonic processing of thermoplastic foam. Polym Eng Sci 30(3):147–152
38. Gandhi A, Asija N, Kumar Gaur K, Rizvi SJA, Tiwari V, Bhatnagar N (2013) Ultrasound assisted cyclic solid-state foaming for fabricating ultra-low density porous acrylonitrile-butadiene-styrene foams. Mater Lett 94:76–78
39. Gandhi A, Bhatnagar N (2015) Significance of ultrasonic cavitation field distribution in microcellular foaming of polymers. Cell Polym 34(1):1–14
40. Lee KM, Lee EK, Kim SG, Park CB, Naguib HE (2009) Bicellular foam structure of polystyrene from extrusion foaming process. J Cell Plast 45(6):539–553
41. Wang Z, Ding X, Zhao M, Wang X, Xu G, Xiang A, Zhou H (2017) A cooling and two-step depressurization foaming approach for the preparation of modified HDPE foam with complex cellular structure. J Supercrit Fluids 125:22–30
42. Zhang C, Zhu B, Li D, Lee LJ (2012) Extruded polystyrene foams with bimodal cell morphology. Polymer. 53(12):2435–2442
43. Bao JB, Liu T, Zhao L, Hu GH (2011) A two-step depressurization batch process for the formation of bi-modal cell structure polystyrene foams using scCO2. J Supercrit Fluids 55(3):1104–1114
44. Bao JB, Weng GS, Zhao L, Liu ZF, Chen ZR (2014) Tensile and impact behavior of polystyrene microcellular foams with bi-modal cell morphology. J Cell Plast 50(4):381–393
45. Ma Z, Zhang G, Yang Q, Shi X, Shi A (2014) Fabrication of microcellular polycarbonate foams with unimodal or bimodal cell-size distributions using supercritical carbon dioxide as a blowing agent. J Cell Plast 50(1):55–79
46. Ma Z, Zhang G, Yang Q, Shi X, Liu Y (2015) Mechanical and dielectric properties of microcellular polycarbonate foams with unimodal or bimodal cell-size distributions. J Cell Plast 51(3):307–327
47. Yu P, Mi HY, Huang A, Geng LH, Chen BY, Kuang TR, Mou WJ, Peng XF (2015) Effect of poly(butylenes succinate) on poly(lactic acid) foaming behavior: formation of open cell structure. Ind Eng Chem Res 54(23):6199–6207
48. Wang X, Wang W, Liu B, Du Z, Peng X (2016) Complex cellular structure evolution of polystyrene/poly (ethylene terephthalate glycol-modified) foam using a two-step depressurization batch foaming process. J Cell Plast 52(6):595–618
49. Li C, Feng LF, Gu XP, Cao K, Zhang CL (2018) In situ visualization on formation mechanism of bi-modal foam via a two-step depressurization approach. J Supercrit Fluids 135:8–16
50. Chen CX, Peng HH, Guan YX, Yao SJ (2019) Morphological study on the pore growth profile of poly(ε-caprolactone) bi-

modal porous foams using a modified supercritical CO2 foaming process. J Supercrit Fluids 143:72–81
51. Arora KA, Lesser AJ, McCarthy TJ (1998) Preparation and characterization of microcellular polystyrene foams processed in supercritical carbon dioxide. Macromolecules. 31(14):4614–4620
52. Zhang C, Zhu B, Lee LJ (2011) Extrusion foaming of polystyrene/carbon particles using carbon dioxide and water as co-blowing agents. Polymer. 52(8):1847–1855
53. Nistor A, Topiar M, Sovova H, Kosek J (2017) Effect of organic co-blowing agents on the morphology of CO2 blown microcellular polystyrene foams. J Supercrit Fluids 130:30–39
54. Daigneault LE, Gendron R (2001) Blends of CO2 and 2-ethyl hexanol as replacement foaming agents for extruded polystyrene. J Cell Plast 37(3):262–272
55. Jiang XL, Tao Liu, Zhao L, Xu ZM, Yuan WK. Effects of blend morphology on the foaming of polypropylene/ low-density polyethylene blends during a batch foaming process. J Cell Plast 2009;45(3):225–241
56. Tang L, Zhai W, Zheng W (2011) Autoclave preparation of expanded polypropylene/poly(lactic acid) blend bead foams with a batch foaming process. J Cell Plast 47(5):429–446
57. Kohlhoff D, Nabil A, Ohshima M (2012) In situ preparation of cross-linked polystyrene/poly(methyl methacrylate) blend foams with a bimodal cellular structure. Polym Adv Technol 23(10): 1350–1356
58. Wang K, Pang Y, Wu F, Zhai W, Zheng W (2016) Cell nucleation in dominating formation of bimodal cell structure in polypropylene/polystyrene blend foams prepared via continuous extrusion with supercritical CO2. J Supercrit Fluids 110:65–74
59. Huang J-N, Jing X, Geng L-H, Chen B-Y, Mi H-Y, Peng X-F (2015) A novel multiple soaking temperature (MST) method to prepare polylactic acid foams with bi-modal open-pore structure and their potential in tissue engineering applications. J Supercrit Fluids 103:28–37
60. Xu LQ, Huang HX (2016) Formation mechanism and tuning for bi-modal cell structure in polystyrene foams by synergistic effect of temperature rising and depressurization with supercritical CO2. J Supercrit Fluids 109:177–185
61. Radhakrishna G, Dugad R, Gandhi A. Bimodal Microcellular Morphology Evaluation in ABS-Foamed Composites Developed Using Step-Wise Depressurization Foaming Process. Polym Eng Sci. 2019;pen.25265
62. Bernardo V, Martin-de Leon J, Pinto J, Verdejo R, Rodriguez-Perez MA (2019) Modeling the heat transfer by conduction of nanocellular polymers with bimodal cellular structures. Polymer. 160:126–137
63. Gandhi A, Panda R, Mohanty S, Nayak SK (2019) Microstructure assessment of bi-modal microcellular polymeric composites developed using multi-stage depressurisation technique in solid-state foaming technology. Int J Microstruct Mater Prop 14(3):226
64. Dugad R, Radhakrishna G, Gandhi A (2019) Morphological evaluation of ultralow density microcellular foamed composites developed through CO_2 -induced solid-state batch foaming technique utilizing water as co-blowing agent. Cell Polym 31: 026248931989763
65. Cho S, Cha SW, Seo J, Ahn J (2013) A study on the foaming ratio and optical characteristics of microcellular foamed plastics produced by a repetitive foaming process. Int J Precis Eng Manuf 14(7):1147–1152
66. Seo J-H, Ohm W-S, Cho S-H, Cha SW (2011) Effects of repeated microcellular foaming process on cell morphology and foaming ratio of microcellular plastics. Polym-Plast Technol Eng 50(6): 588–592
67. Nawaby AV, Handa YP (2003) The second expansion cycle in ultramicrocellular foams. Cell Polym 22(4):260–268
68. Radhakrishna G, Dugad R, Gandhi A, Mohanty S, Nayak SK (2019) Morphological evaluation of ultra low-density poly (methyl methacrylate) microcellular plastic developed through cyclic foaming technique. Int J Mater Eng Innov 10(4):310
69. Sankaran S, Deshmukh K, Ahamed MB, Khadheer Pasha SK (2018) Recent advances in electromagnetic interference shielding properties of metal and carbon filler reinforced flexible polymer composites: A review. Compos Part A Appl Sci Manuf 114:49–71
70. Singh AK, Shishkin A, Koppel T, Gupta N (2018) A review of porous lightweight composite materials for electromagnetic interference shielding. Compos Part B Eng 149:188–197
71. Jiang D, Murugadoss V, Wang Y, Lin J, Ding T, Wang Z, Shao Q, Wang C, Liu H, Lu N, Wei R, Subramania A, Guo Z (2019) Electromagnetic interference shielding polymers and Nanocomposites - A review. Polym Rev 59(2):280–337
72. Lu D, Mo Z, Liang B, Yang L, He Z, Zhu H, Tang Z, Gui X (2018) Flexible, lightweight carbon nanotube sponges and composites for high-performance electromagnetic interference shielding. Carbon NY 133:457–463
73. Huang J-C (1995) EMI shielding plastics: A review. Adv Polym Technol 14(2):137–150
74. Xu L, Jia LC, Yan DX, Ren PG, Xu JZ, Li ZM (2018) Efficient electromagnetic interference shielding of lightweight carbon nanotube/polyethylene composites: via compression molding plus salt-leaching. RSC Adv 8(16):8849–8855
75. Ling J, Zhai W, Feng W, Shen B, Zhang J, Zheng WG (2013) Facile preparation of lightweight microcellular polyetherimide/graphene composite foams for electromagnetic interference shielding. ACS Appl Mater Interfaces 5(7):2677–2684
76. Thomassin JM, Vuluga D, Alexandre M, Jérôme C, Molenberg I, Huynen I, Detrembleur C (2012) A convenient route for the dispersion of carbon nanotubes in polymers: application to the preparation of electromagnetic interference (EMI) absorbers. Polymer. 53(1):169–174
77. Xu X, Bin LZM, Shi L, Bian XC, Xiang ZD (2007) Ultralight conductive carbon-nanotube-polymer composite. Small. 3(3): 408–411
78. Wang G, Zhao G, Wang S, Zhang L, Park CB (2018) Injection-molded microcellular PLA/graphite nanocomposites with dramatically enhanced mechanical and electrical properties for ultra-efficient EMI shielding applications. J Mater Chem C 6(25): 6847–6859
79. Yang Y, Gupta MC, Dudley KL, Lawrence RW (2005) Novel carbon nanotube - polystyrene foam composites for electromagnetic interference shielding. Nano Lett 5(11):2131–2134
80. Yan D-X, Ren P-G, Pang H, Fu Q, Yang M-B, Li Z-M (2012) Efficient electromagnetic interference shielding of lightweight graphene/polystyrene composite. J Mater Chem 22(36):18772
81. Zhang H-B, Yan Q, Zheng W-G, He Z, Yu Z-Z (2011) Tough Graphene−polymer microcellular foams for electromagnetic interference shielding. ACS Appl Mater Interfaces 3(3):918–924
82. Shen B, Zhai W, Tao M, Ling J, Zheng W (2013) Lightweight, multifunctional polyetherimide/graphene@Fe3O 4 composite foams for shielding of electromagnetic pollution. ACS Appl Mater Interfaces 5(21):11383–11391
83. Shen B, Li Y, Zhai W, Zheng W (2016) Compressible Graphene-coated polymer foams with ultralow density for adjustable electromagnetic interference (EMI) shielding. ACS Appl Mater Interfaces 8(12):8050–8057
84. Zeng Z, Jin H, Chen M, Li W, Zhou L, Zhang Z (2016) Lightweight and anisotropic porous MWCNT/WPU composites for ultrahigh performance electromagnetic interference shielding. Adv Funct Mater 26(2):303–310
85. Ameli A, Jung PU, Park CB (2013) Electrical properties and electromagnetic interference shielding effectiveness of polypropylene/carbon fiber composite foams. Carbon NY 60:379–391

86. Bernal MM, Molenberg I, Estravis S, Rodriguez-Perez MA, Huynen I, Lopez-Manchado MA, Verdejo R (2012) Comparing the effect of carbon-based nanofillers on the physical properties of flexible polyurethane foams. J Mater Sci 47(15):5673–5679
87. Ameli A, Nofar M, Wang S, Park CB (2014) Lightweight polypropylene/stainless-steel fiber composite foams with low percolation for efficient electromagnetic interference shielding. ACS Appl Mater Interfaces 6(14):11091–11100
88. Xu Y, Xu W, Bao J (2014) A high performance electromagnetic interference shielding epoxy composite with multiple conductive networks in the matrix. J Polym Res 21(8):1–8
89. Lakes R (1987) Foam structures with a negative Poisson's ratio. Science. 235(4792):1038–1040
90. Saxena KK, Das R, Calius EP (2016) Three decades of Auxetics research − materials with negative Poisson's ratio: A review. Adv Eng Mater 18(11):1847–1870
91. Liu Y, Hu H (2010) A review on auxetic structures and polymeric materials. Sci Res Essays 5(10):1052–1063
92. Carneiro VH, Meireles J, Puga H (2013) Auxetic materials - A review. Mater Sci Pol 31(4):561–571
93. Alderson A, Alderson KL (2007) Auxetic materials. Proc Inst Mech Eng Part G J Aerosp Eng 221(4):565–575
94. Yang W, Li Z-M, Shi W, Xie B-H, Yang M-B (2004) Review on auxetic materials. J Mater Sci 39(10):3269–3279
95. Ren X, Das R, Tran P, Ngo TD, Xie YM (2018) Auxetic metamaterials and structures: A review. Smart Mater Struct 27(2): 023001
96. Yousif Yousif HI, Mohammed EL-Butch A, EL-Mahdy TH, Zied KM. Auxetic Polyurethane Foam (Fabrication, Properties and Applications). Nuclear Research Helwan University (Egypt); 2012
97. Critchley R, Corni I, Wharton JA, Walsh FC, Wood RJK, Stokes KR (2013) A review of the manufacture, mechanical properties and potential applications of auxetic foams. Phys Status Solidi Basic Res 250(10):1963–1982
98. Novak N, Vesenjak M, Ren Z (2016) Auxetic cellular materials - A review. Aust J Mech Eng 62(9):485–493
99. Sanami M, Ravirala N, Alderson K, Alderson A (2014) Auxetic materials for sports applications. Procedia Eng 72:453–458
100. Bianchi M, Frontoni S, Scarpa F, Smith CW (2011) Density change during the manufacturing process of PU-PE open cell auxetic foams. Phys Status Solidi 248(1):30–38
101. Wang YC, Lakes R, Butenhoff A (2001) Influence of cell size on re-entrant transformation of negative Poisson's ratio reticulated polyurethane foams. Cell Polym 20(4–6):373–385
102. Yao Y, Luo Y, Xu Y, Wang B, Li J, Deng H, Lu H (2018) Fabrication and characterization of auxetic shape memory composite foams. Compos Part B Eng 152:1–7
103. Alderson K, Alderson A, Ravirala N, Simkins V, Davies P (2012) Manufacture and characterisation of thin flat and curved auxetic foam sheets. Phys Status Solidi Basic Res 249(7):1315–1321
104. Grima JN, Attard D, Gatt R, Cassar RN (2009) A novel process for the manufacture of Auxetic foams and for their re-conversion to conventional form. Adv Eng Mater 11(7):533–535
105. Bianchi M, Scarpa F, Banse M, Smith CW (2011) Novel generation of auxetic open cell foams for curved and arbitrary shapes. Acta Mater 59(2):686–691
106. Fan D, Li M, Qiu J, Xing H, Jiang Z, Tang T (2018) Novel method for preparing Auxetic foam from closed-cell polymer foam based on the steam penetration and condensation process. ACS Appl Mater Interfaces 10(26):22669–22677
107. Quadrini F, Bellisario D, Ciampoli L, Costanza G, Santo L (2016) Auxetic epoxy foams produced by solid state foaming. J Cell Plast 52(4):441–454
108. Chan N, Evans KE (1997) Fabrication methods for auxetic foams. J Mater Sci 32(22):5945–5953
109. Dehghani F, Annabi N (2011) Engineering porous scaffolds using gas-based techniques. Curr Opin Biotechnol 22(5):661–666
110. Zhao P, Gu H, Mi H, Rao C, Fu J, Turng L (2018) Sheng. Fabrication of scaffolds in tissue engineering: A review. Front Mech Eng 13(1):107–119
111. Mi HY, Jing X, Turng LS (2014) Fabrication of porous synthetic polymer scaffolds for tissue engineering. J Cell Plast 51(2):165–196
112. Cooper AI (2003) Porous materials and supercritical fluids. Adv Mater 15(13):1049–1059
113. Huang C, Thomas NL (2018) Fabricating porous poly(lactic acid) fibres via electrospinning. Eur Polym J 99:464–476
114. Qin Z, Zhang P, Wu Z, Yin M, Geng Y, Pan K (2018) Coaxial electrospinning for flexible uniform white-light-emitting porous fibrous membrane. Mater Des 147:175–181
115. Xu T, Liang Z, Ding B, Feng Q, Fong H (2018) Polymer blend nanofibers containing polycaprolactone as biocompatible and biodegradable binding agent to fabricate electrospun three-dimensional scaffolds/structures. Polymer. 151:299–306
116. Dhandayuthapani B, Yoshida Y, Maekawa T, Kumar DS (2011) Polymeric scaffolds in tissue engineering application: A review. Int J Polym Sci 2011:1–19
117. Mohanty S, Sanger K, Heiskanen A, Trifol J, Szabo P, Dufva M, Emnéus J, Wolff A (2016) Fabrication of scalable tissue engineering scaffolds with dual-pore microarchitecture by combining 3D printing and particle leaching. Mater Sci Eng C 61:180–189
118. Seleznev VA, Prinz VY (2017) Hybrid 3D–2D printing for bone scaffolds fabrication. Nanotechnology. 28(6):064004
119. Mancuso E, Alharbi N, Bretcanu OA, Marshall M, Birch MA, McCaskie AW et al (2017) Three-dimensional printing of porous load-bearing bioceramic scaffolds. Proc Inst Mech Eng Part H J Eng Med 231(6):575–585
120. Jakus AE, Secor EB, Rutz AL, Jordan SW, Hersam MC, Shah RN (2015) Three-dimensional printing of high-content graphene scaffolds for electronic and biomedical applications. ACS Nano 9(4): 4636–4648
121. Zein I, Hutmacher DW, Tan KC, Teoh SH (2002) Fused deposition modeling of novel scaffold architectures for tissue engineering applications. Biomaterials. 23(4):1169–1185
122. Wang X, Salick MR, Gao Y, Jiang J, Li X, Liu F, Cordie T, Li Q, Turng LS (2018) Interconnected porous poly(ε-caprolactone) tissue engineering scaffolds fabricated by microcellular injection molding. J Cell Plast 54(2):379–397
123. Aram E, Mehdipour-Ataei S (2016) A review on the micro- and nanoporous polymeric foams: preparation and properties. Int J Polym Mater Polym Biomater 65(7):358–375
124. Huang A, Mi H, Peng X, Jiang Y, Turng L-S, Napiwocki B (2017) Fabrication of poly(ϵ-caprolactone) tissue engineering scaffolds with fibrillated and interconnected pores utilizing microcellular injection molding and polymer leaching. RSC Adv 7(69): 43432–43444
125. Jing X, Mi HY, Cordie T, Salick M, Peng XF, Turng LS (2014) Fabrication of porous poly(ε-caprolactone) scaffolds containing chitosan nanofibers by combining extrusion foaming, leaching, and freeze-drying methods. Ind Eng Chem Res 53(46):17909–17918
126. Gandhi A, Bhatnagar N (2015) Surface quenching induced microstructure transformations in extrusion foaming of porous sheets. Int Polym Process 30(3):397–402
127. Jaganathan SK, Mani MP, Palaniappan SK, Rathanasamy R (2018) Fabrication and characterisation of nanofibrous polyurethane scaffold incorporated with corn and neem oil using single stage electrospinning technique for bone tissue engineering applications. J Polym Res 25(7):1–12
128. Thakare VG, Joshi PA, Godse RR, Bhatkar VB, Wadegaokar PA, Omanwar SK (2017) Fabrication of polycaprolactone/zirconia

nanofiber scaffolds using electrospinning technique. J Polym Res 24(12):1–11
129. Matuana LM, Diaz CA (2010) Study of cell nucleation in microcellular poly(lactic acid) foamed with supercritical CO_2 through a continuous-extrusion process. Ind Eng Chem Res 49(5):2186–2193
130. Gomes ME, Godinho JS, Tchalamov D, Cunha AM, Reis RL (2002) Alternative tissue engineering scaffolds based on starch: processing methodologies, morphology, degradation and mechanical properties. Mater Sci Eng C 20(1–2):19–26
131. Pintado-Sierra M, Delgado L, Aranaz I, Marcos-Fernández Á, Reinecke H, Gallardo A, Zeugolis D, Elvira C (2014) Surface hierarchical porosity in poly (ε-caprolactone) membranes with potential applications in tissue engineering prepared by foaming in supercritical carbon dioxide. J Supercrit Fluids 95:273–284
132. Cuénoud M, Bourban PE, Plummer CJG, Månson JAE (2012) Plasticization of polylactide foams for tissue engineering. J Cell Plast 48(5):409–432
133. Floren M, Spilimbergo S, Motta A, Migliaresi C (2011) Porous poly(D,L-lactic acid) foams with tunable structure and mechanical anisotropy prepared by supercritical carbon dioxide. J Biomed Mater Res Part B Appl Biomater 99B(2):338–349
134. Singh L, Kumar V, Ratner BD (2004) Generation of porous microcellular 85/15 poly (dl-lactide-co-glycolide) foams for biomedical applications. Biomaterials. 25(13):2611–2617
135. Gardner DJ, Han Y, Wang L (2015) Wood–plastic composite technology. Curr For Rep 1(3):139–150
136. Niska KO, Sain M. Wood-Polymer Composites. Wood-Polymer Composites. Woodhead Publishing; 2008. 1–366 p
137. Chan CM, Vandi LJ, Pratt S, Halley P, Richardson D, Werker A, Laycock B (2018) Composites of Wood and biodegradable thermoplastics: A review. Polym Rev 58(3):444–494
138. Matuana LM, Stark NM (2014) The use of wood fibers as reinforcements in composites. Biofiber Reinf Compos Mater 1:648–688
139. Zhang ZX, Zhang J, Lu B-X, Xin ZX, Kang CK, Kim JK (2012) Effect of flame retardants on mechanical properties, flammability and foamability of PP/wood–fiber composites. Compos Part B Eng 43(2):150–158
140. Zhang S, Rodrigue D, Riedl B (2005) Preparation and morphology of polypropylene/wood flour composite foams via extrusion. Polym Compos 26(6):731–738
141. Faruk O, Bledzki AK, Matuana LM (2007) Microcellular foamed Wood-plastic composites by different processes: a review. Macromol Mater Eng 292(2):113–127
142. Li Q, Matuana LM (2003) Foam extrusion of high density polyethylene/wood-flour composites using chemical foaming agents. J Appl Polym Sci 88(14):3139–3150
143. Lee YH, Kuboki T, Park CB, Sain M (2011) The effects of nanoclay on the extrusion foaming of wood fiber/polyethylene nanocomposites. Polym Eng Sci 51(5):1014–1022
144. Bledzki AK, Faruk O (2006) Injection moulded microcellular wood fibre–polypropylene composites. Compos Part A Appl Sci Manuf 37(9):1358–1367
145. Xie B, Cui YH, Xu J, Wang XX, Zhang HH, Zhang ZD (2012) Investigation on microstructure and properties of foamed (wood fiber)/(recycled polypropylene) composites. J Vinyl Addit Technol 18(2):105–112
146. Rizvi GM, Guo G, Park CB, Kim YS (2005) Critical issues in extrusion foaming of plastic/Woodfiber composites. Cell Polym 24(6):347–362
147. Choe H, Sung G, Kim JH (2018) Chemical treatment of wood fibers to enhance the sound absorption coefficient of flexible polyurethane composite foams. Compos Sci Technol 156:19–27
148. Feng A, Wu G, Wang Y, Pan C (2017) Synthesis, preparation and mechanical property of Wood Fiber-reinforced poly(vinyl chloride) composites. J Nanosci Nanotechnol 17(6):3859–3863
149. Yeh SK, Hsieh CC, Chang HC, Yen CCC, Chang YC (2015) Synergistic effect of coupling agents and fiber treatments on mechanical properties and moisture absorption of polypropylene-rice husk composites and their foam. Compos Part A Appl Sci Manuf 68:313–322
150. Zhang Z-X, Gao C, Xin ZX, Kim JK (2012) Effects of extruder parameters and silica on physico-mechanical and foaming properties of PP/wood-fiber composites. Compos Part B Eng 43(4): 2047–2057
151. Koay SC, Subramanian V, Chan MY, Pang MM, Tsai KY, Cheah KH (2018) Preparation and Characterization of Wood Plastic Composite Made Up of Durian Husk Fiber and Recycled Polystyrene Foam. Narayana Namasivayam S, Hosseini Fouladi M, Eunice Phang SW, Chua BL, Chow YH, Yong LC, et al., editors. MATEC Web Conf 152:–02019
152. Tawfik ME, Eskander SB, Nawwar GA (2017) Hard wood-composites made of rice straw and recycled polystyrene foam wastes. J Appl Polym Sci 10:134(18)
153. Chun KS, Subramaniam V, Yeng CM, Meng PM, Ratnam CT, Yeow TK et al (2018) Wood plastic composites made from post-used polystyrene foam and agricultural waste. J Thermoplast Compos Mater 13:089270571879983
154. Rachtanapun P, Selke SEM, Matuana LM (2003) Microcellular foam of polymer blends of HDPE/PP and their composites with wood fiber. J Appl Polym Sci 88(12):2842–2850
155. Mengeloglu F, Matuana LM (2001) Foaming of rigid PVC/wood-flour composites through a continuous extrusion process. J Vinyl Addit Technol 7(3):142–148
156. Khoshnoud P, Abu-Zahra N (2017) Properties of rigid polyvinyl chloride foam composites reinforced with different shape fillers. J Thermoplast Compos Mater 30(11):1541–1559